ATLAS Detector

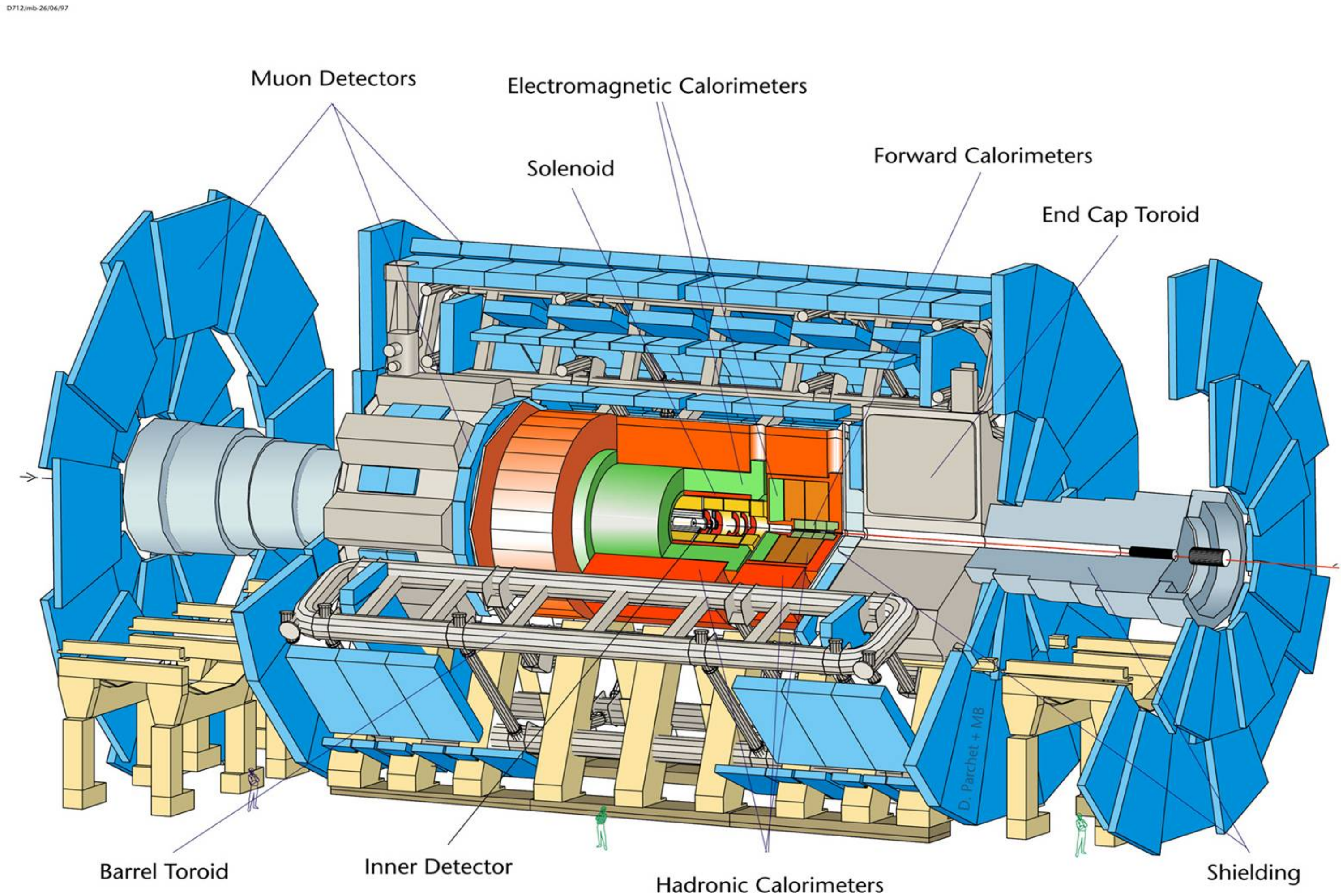

Diameter 25 m
Barrel toroid length 26 m
End-cap end-wall chamber span 46 m
Overall weight 7000 Tons

ATLAS Components (starting from the center/beam line)

Tracker system to measure trajectories of outgoing particles:

Pixels: 140 million pixels 50 x 50 x 300 mm (digital)

Si strips: 6.2 million channels 8 mm x 12.8 cm (digital)

Straws: 420,000 channels 4 mm x 108 cm (digital+analog)

\+ IBL insertable B layer: 26880 pixels, 50 × 250 μm at radius 3.3 cm

Solenoid magnet with 4 Tesla field encloses the tracker

Electromagnetic Calorimeter to identify electrons and photons and measure their energies

Barrel and 2 endcaps 220,000 channels (analog)

Hadronic Calorimeter to identify pions, kaons and protons and to measure their energies

PMT readout, 10,000 channels (analog)

Muon system to identify muons and measure their momentum

4 technologies, 12,000 m^2 covered with 50 mm position resolution, 1.232 million channels (digital)

Toroid magnet systems (barrel+2 endcaps) enclose muon chambers with 0.8 Tesla field.

Luminosity detectors – ZDC, ALPHA, TOTEM,…….

UX15 cavern

Tile (hadronic) calorimeter

First toroid coil

Barrel electromagnetic calorimeter

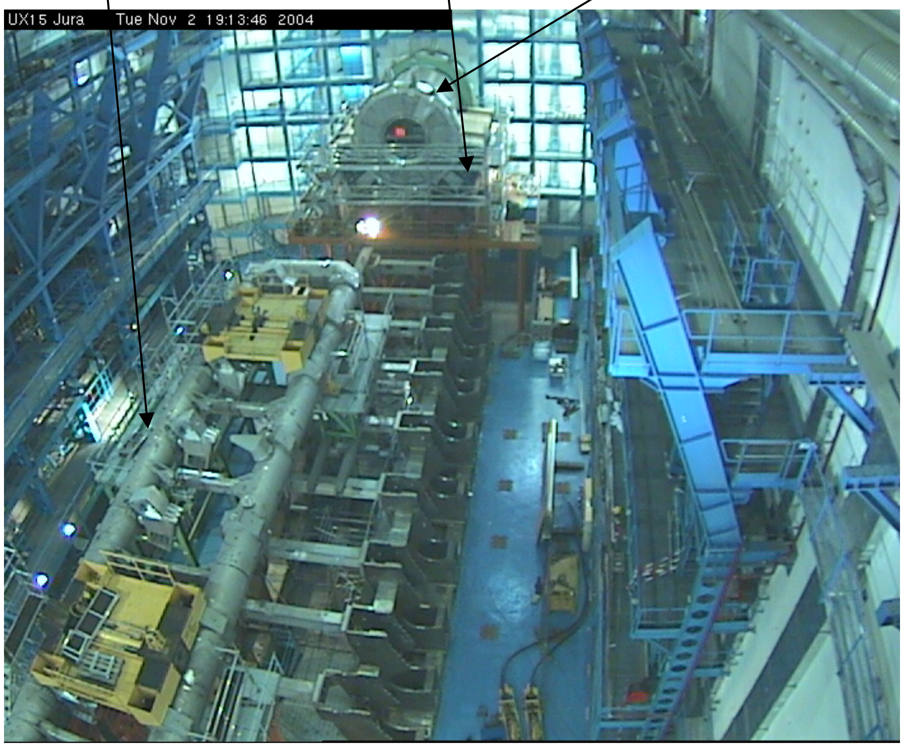

November 2003

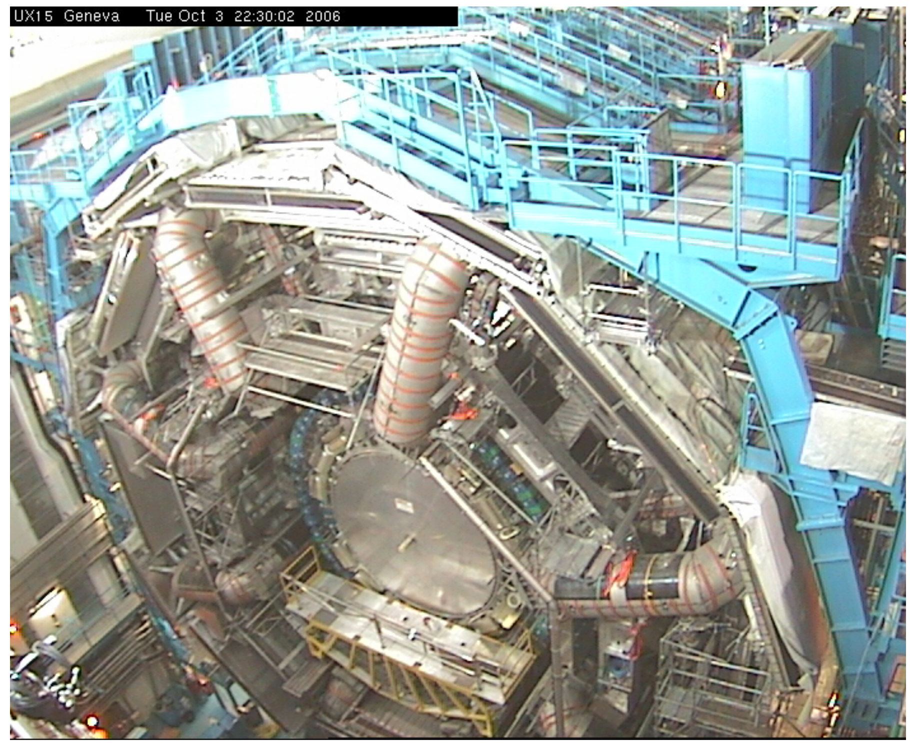

October 2006

Detector (ID)

The Inner Detector (ID) is organized into four sub-systems:

- **Pixels**
- **Silicon Tracker (SCT)**
- **Transition Radiation Tracker (TRT)**
- **Common ID items**

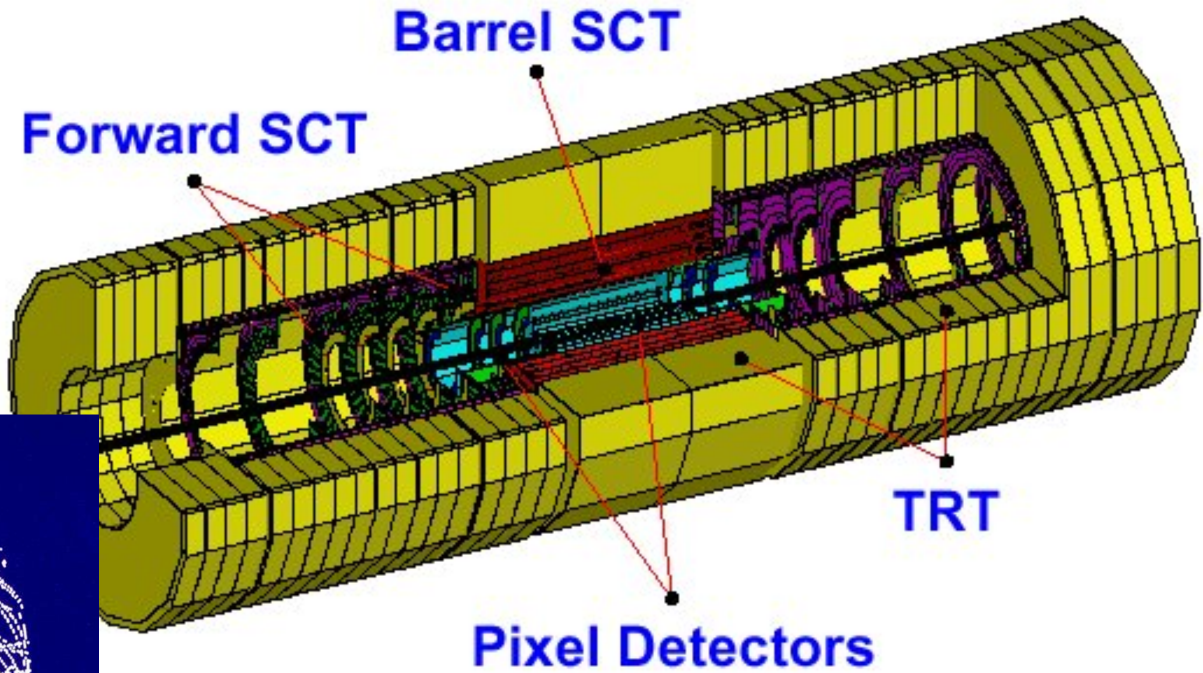

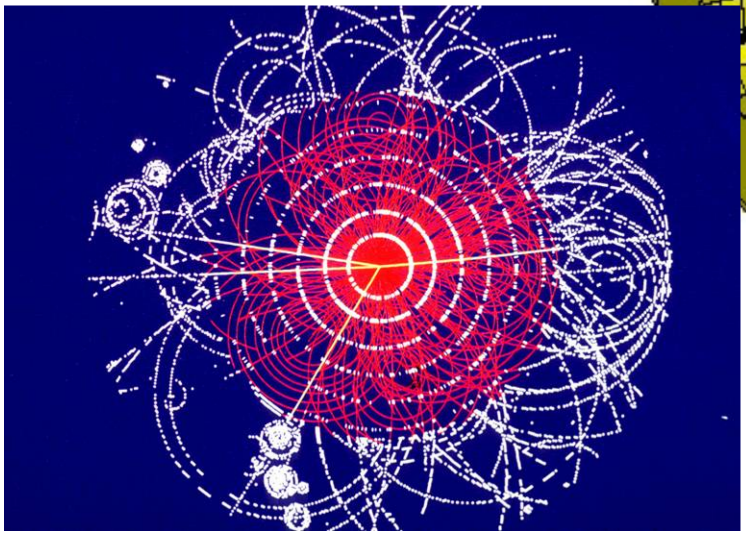

Lot of progress on the Pixels!

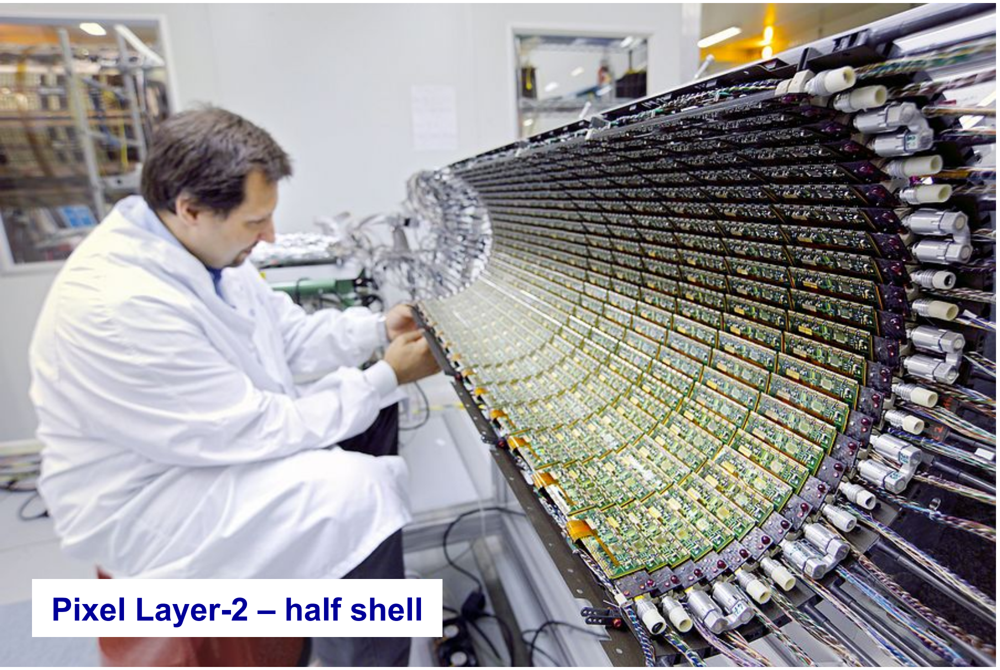

Pixel Layer-2 – half shell

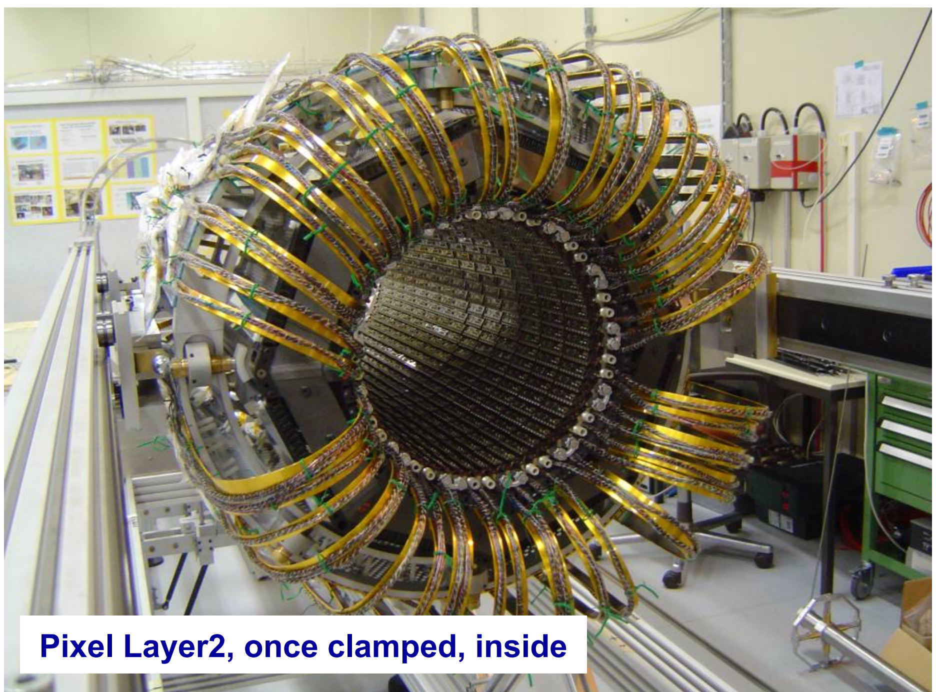

Pixel Layer2, once clamped, inside

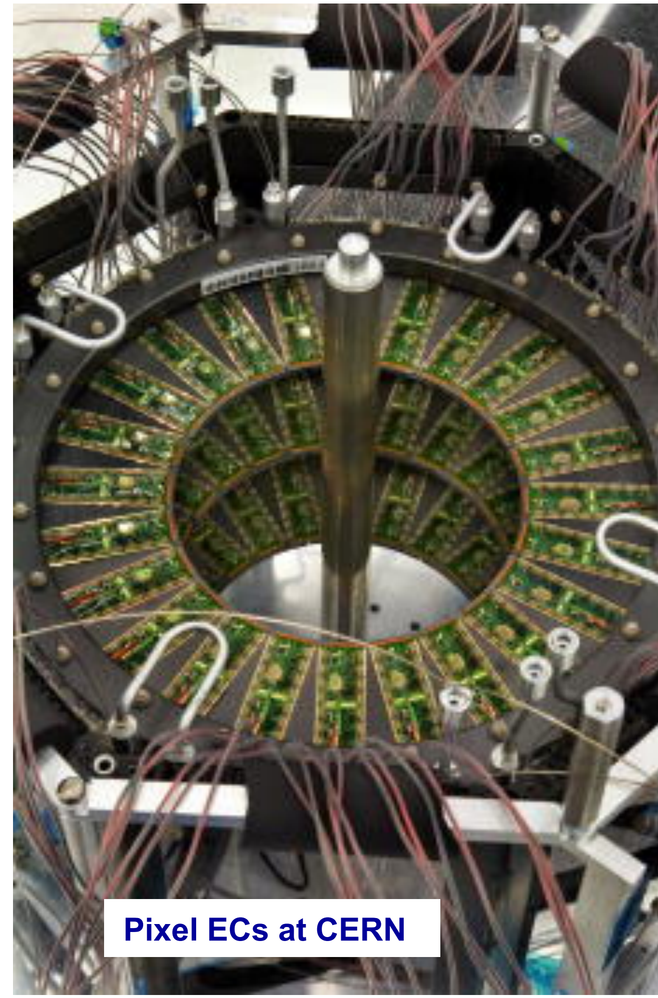

Pixel ECs at CERN

ATLAS **T**ransition **R**adiation **T**racker

A prototype
endcap “wheel”.

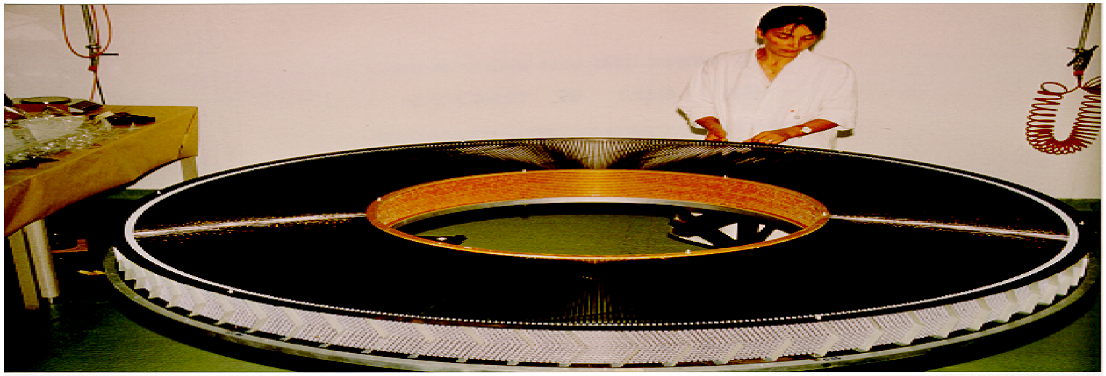

X-ray detector:
straw tubes (4mm)
(in total ca.
400.000 !)

TRT prototype performance
Xe based gas

Pion fake rate
at 90% electron
detection efficiency:

p_{90} = 1.58 %

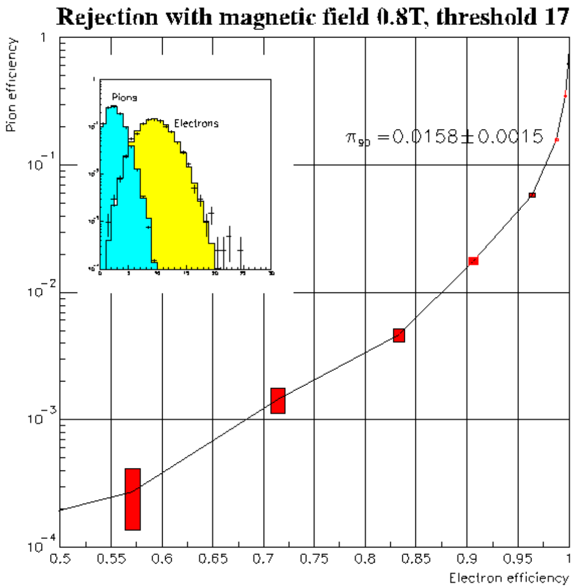

LAr Calorimetry

The LAr calorimetry (pre-samplers, EM, hadronic end-caps, and forward calorimeters)

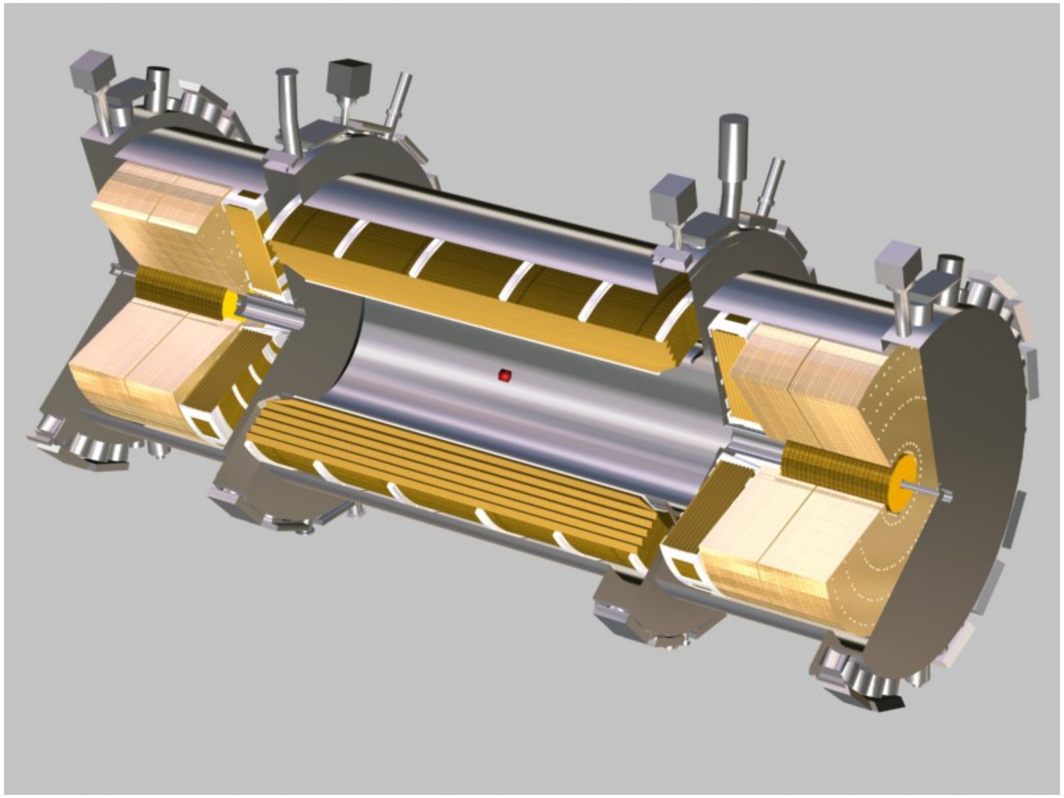

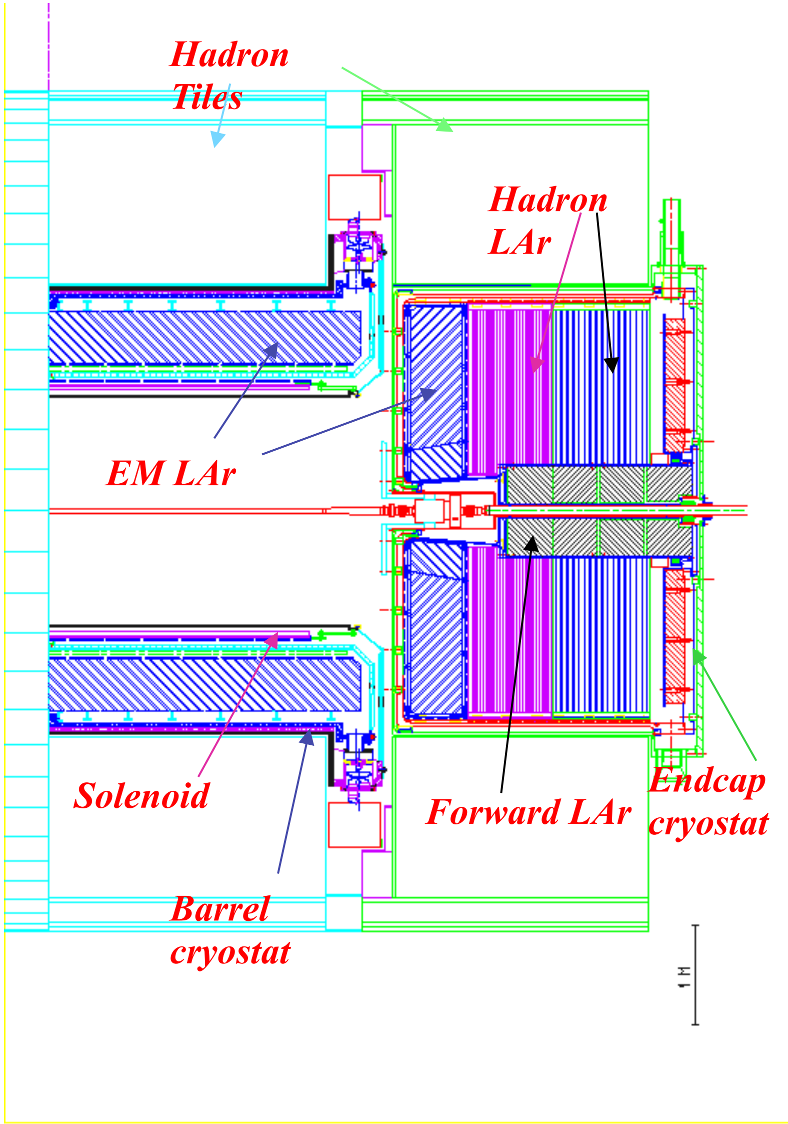

Calorimeters

Electromagnetic calorimeter - Liquid Argon detector with accordion geometry

- **housed in 3 cryostats: barrel + 2 endcaps**
- **barrel section – presampler + 3 radial segments**
- **endcap section – 1.4< h <2.5 3 segments**
  - **2.5< h <3.2 2 segments**

Hadronic calorimeter > 11 l

- **Fe-scintillator barrel**
  - **LAr hadronic endcap**
  - **LAr –W/Cu Forward**

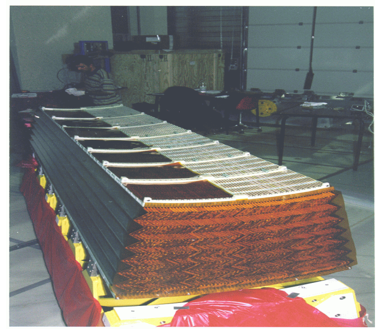

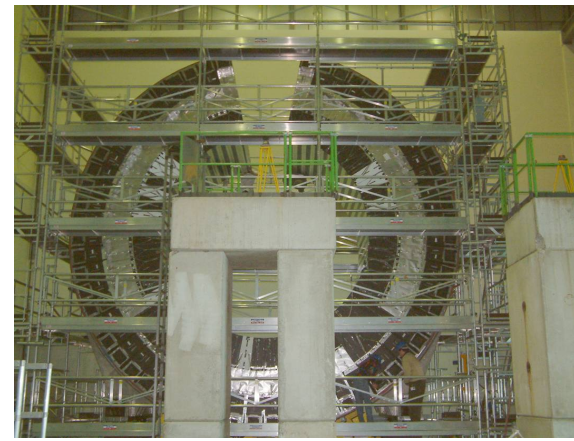

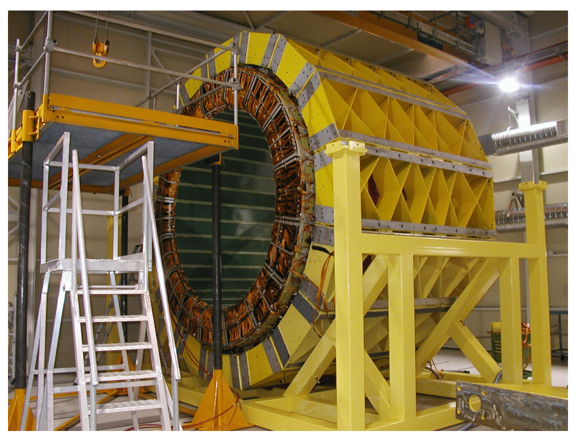

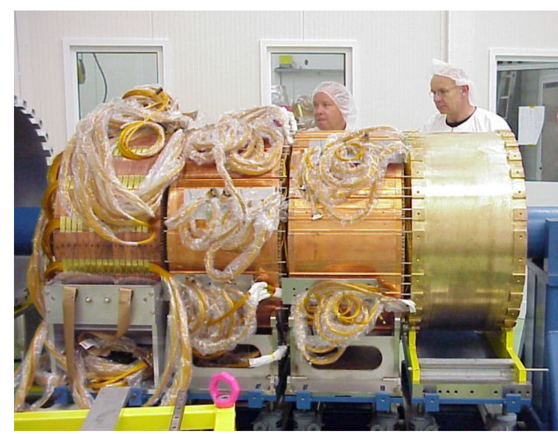

ATLAS LAr End-Cap Calorimeters

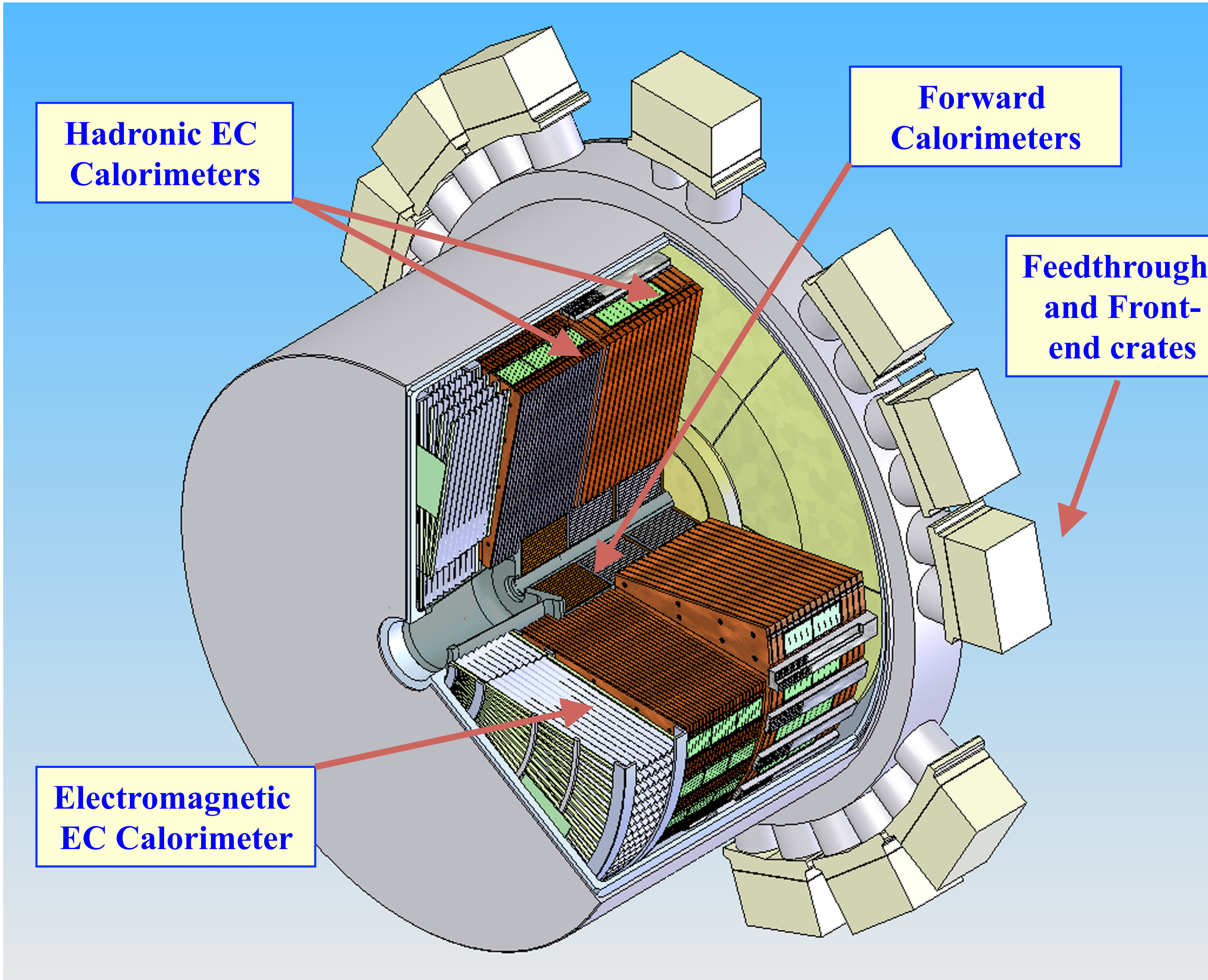

End-Cap Calorimeter C

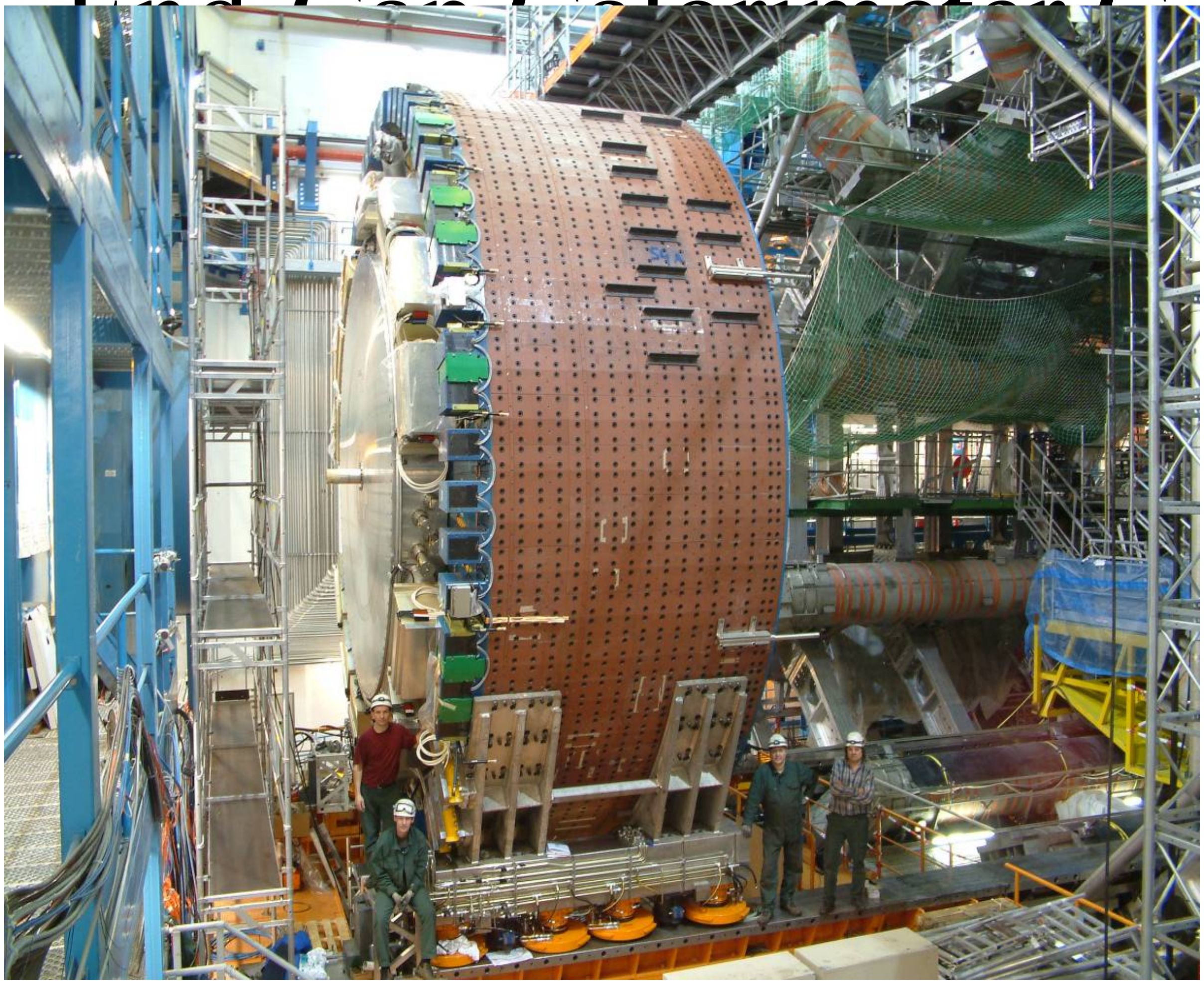

Completed end-cap calorimeter side C, just before insertion into the detector

TRT+SCT barrel travelled to the pit, 24th Aug 2006

Through the parking area

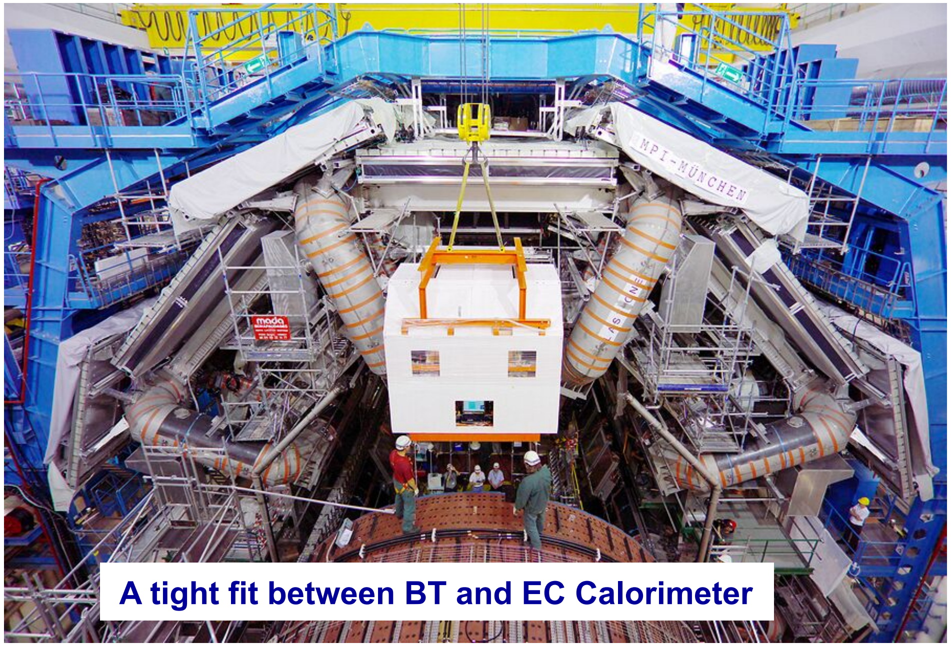

A tight fit between BT and EC Calorimeter

From the trolley to the support rails

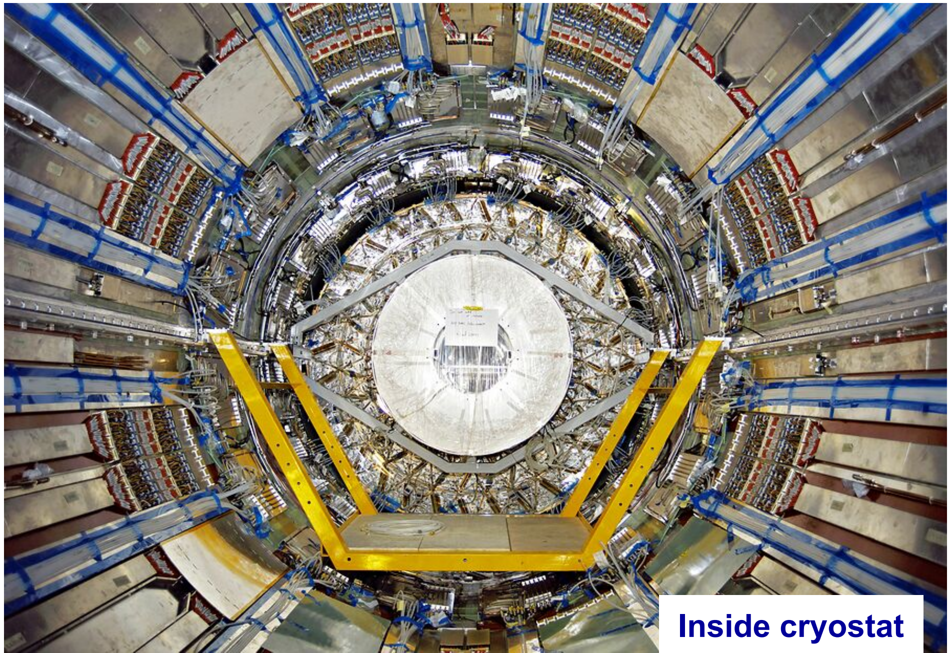

Inside cryostat

Toroid Magnet

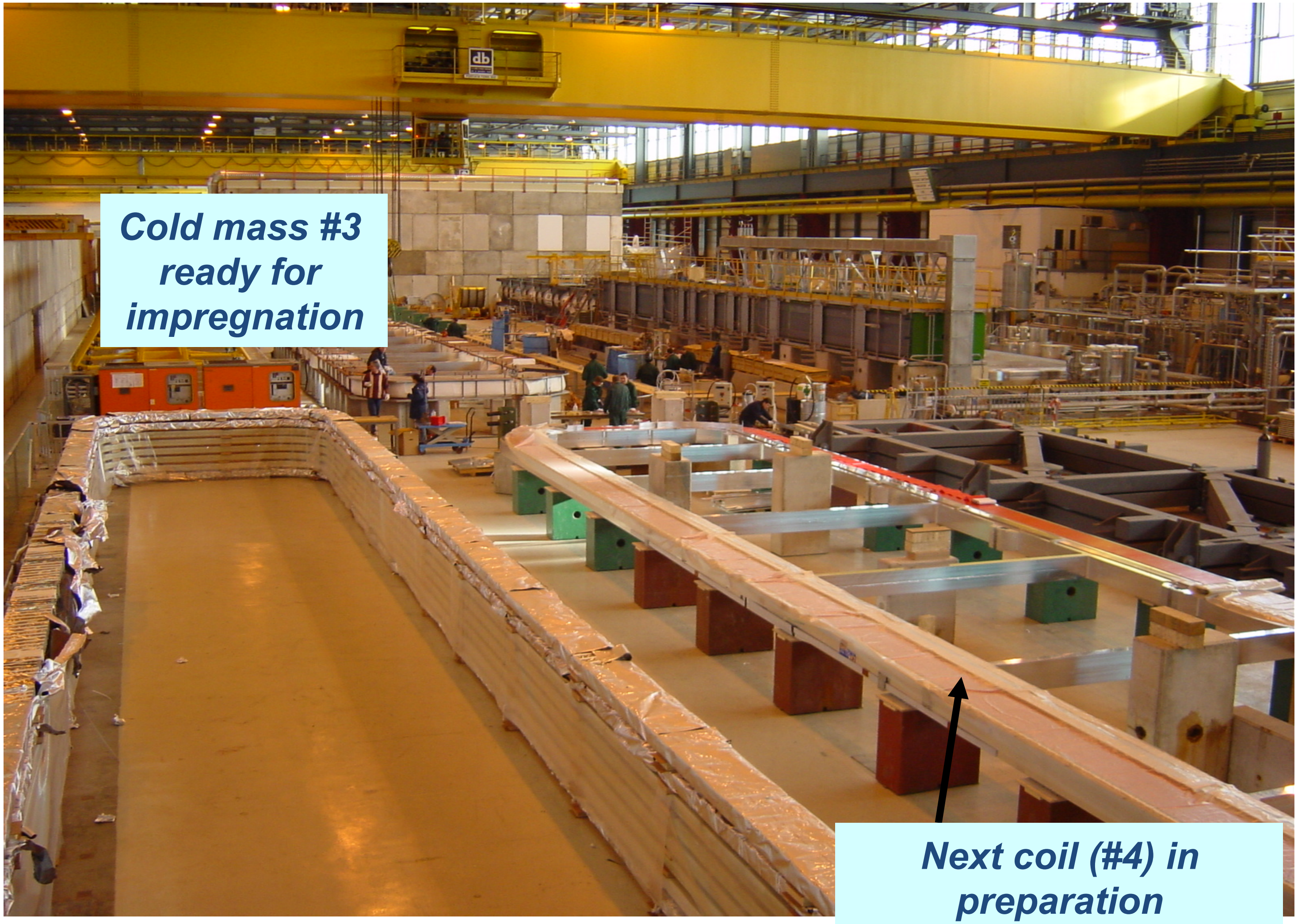

One more view of the first installed TGC Big Wheel

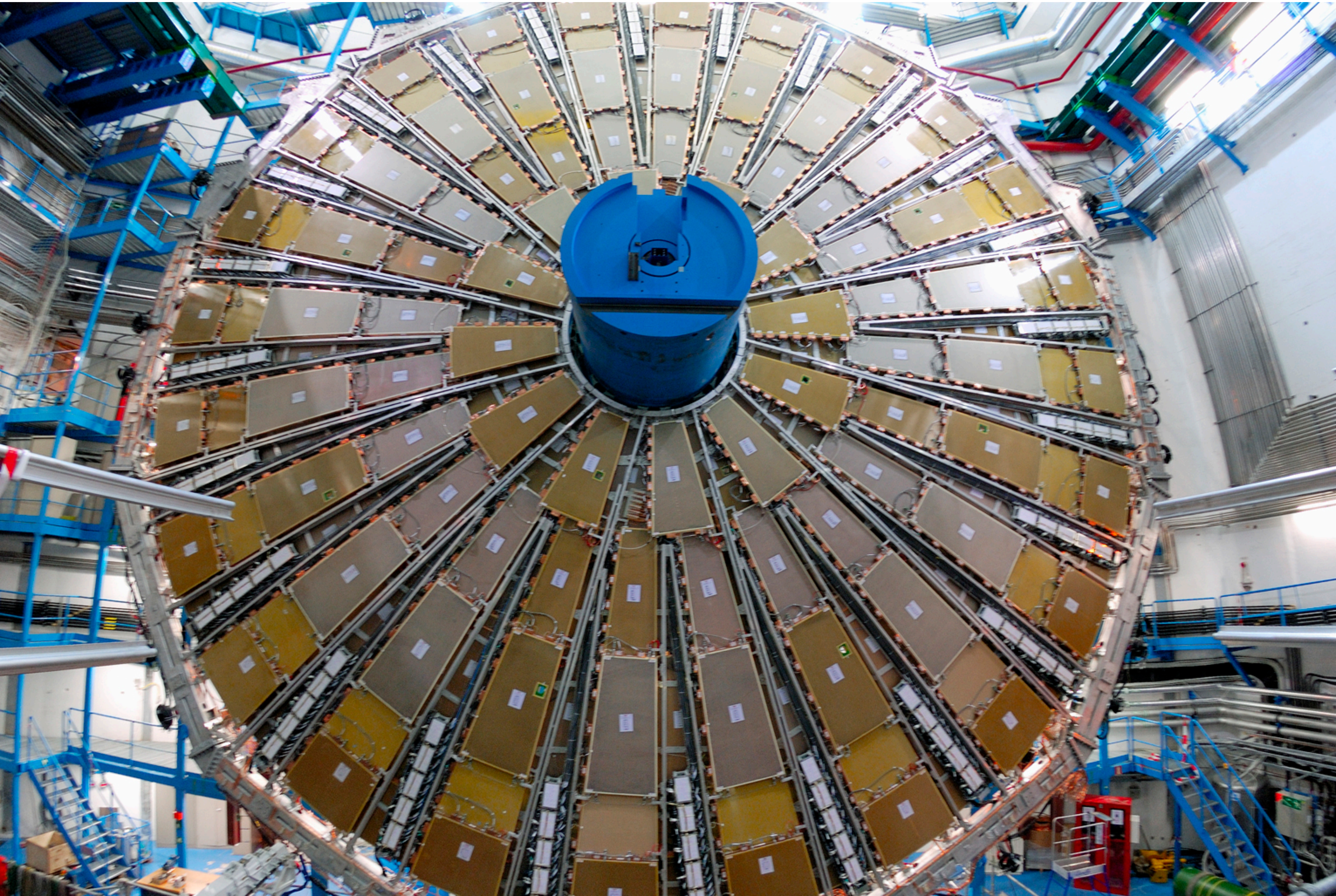

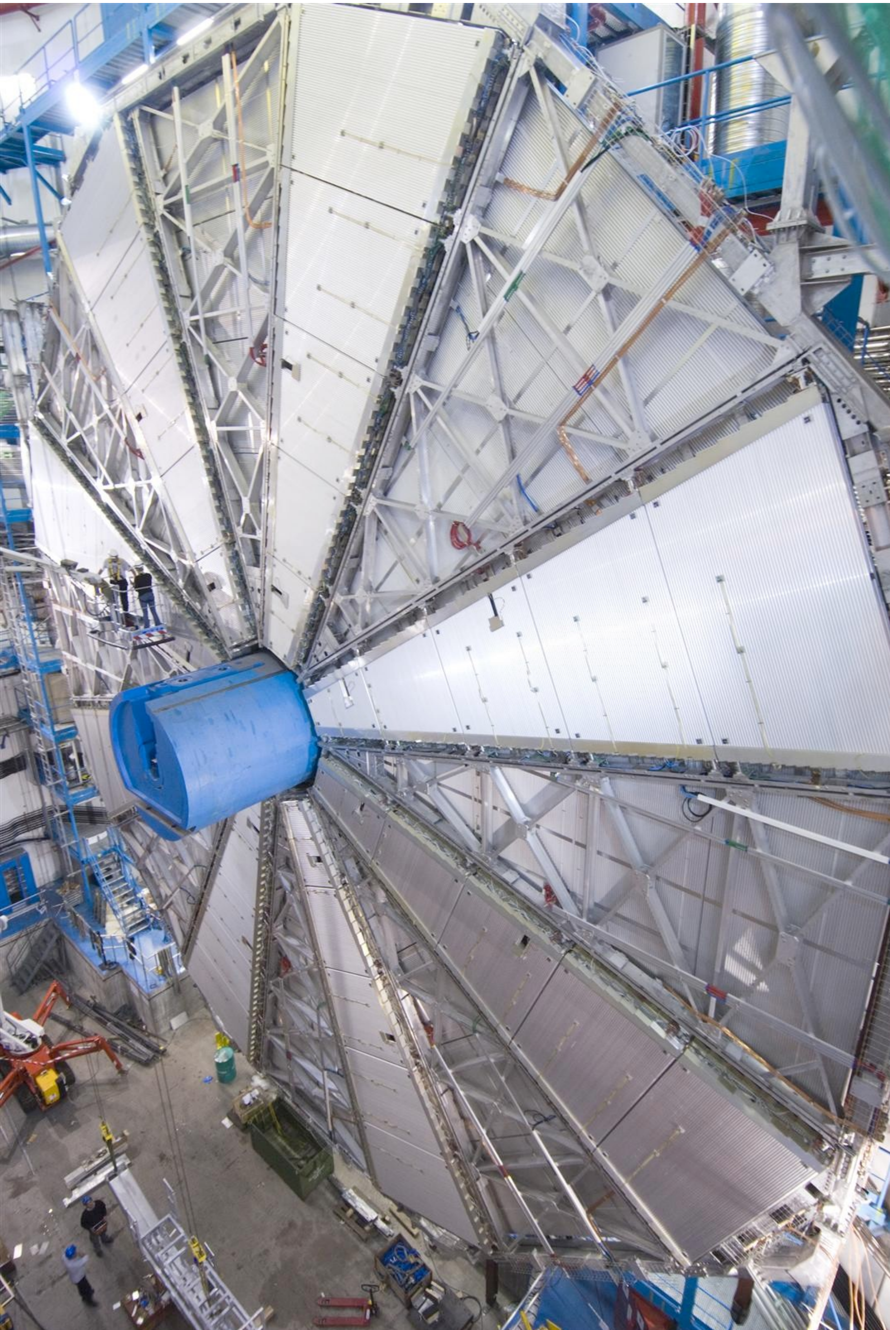

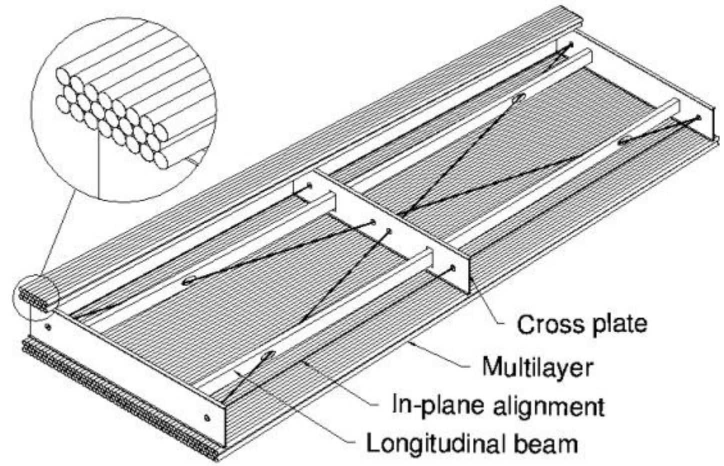

nnot be displayed. Your computer may not have enough memory to open the image, or the image may have been corrupted. Restart your computer, and then open the file again. If the red x still appears, you may have image and then insert it again.

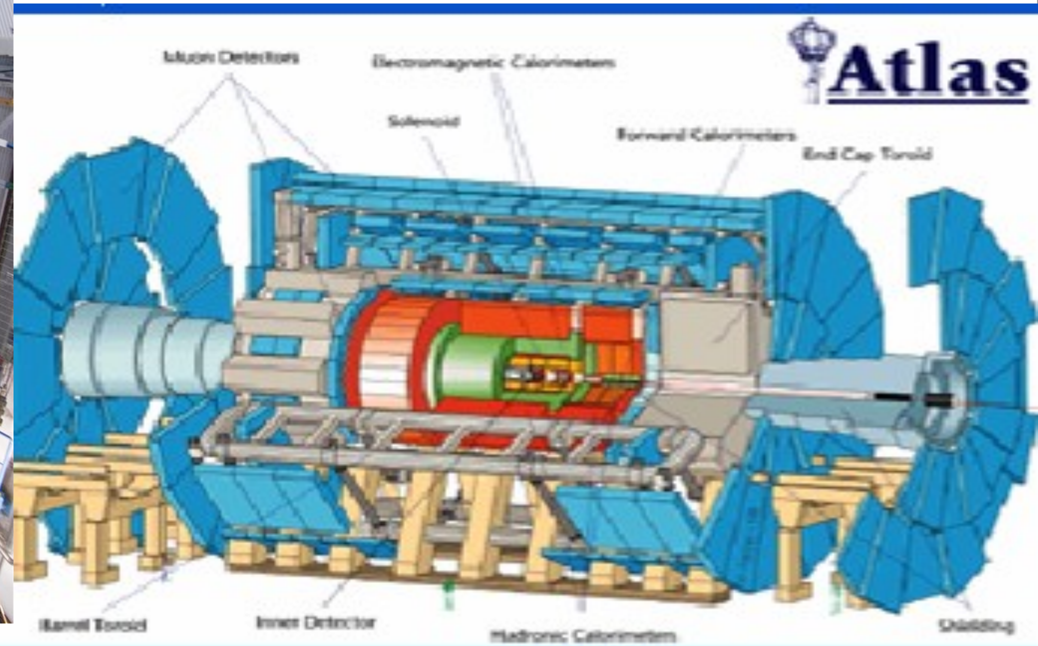

Energy loss dE/dx

- Common features:
  - fast growth, as **1**/β^2, at low energy
  - wide minimum in the range $3 \leq \beta\gamma$
  - slow increase at high $\beta\gamma$
- A particle with
  the minimum is a minimum-ionizing particle or **mip**
- The
  for all materials except hydrogen are in the range 1-2 MeV/(g/cm²)
  - increasing from large to low Z of the absorber.

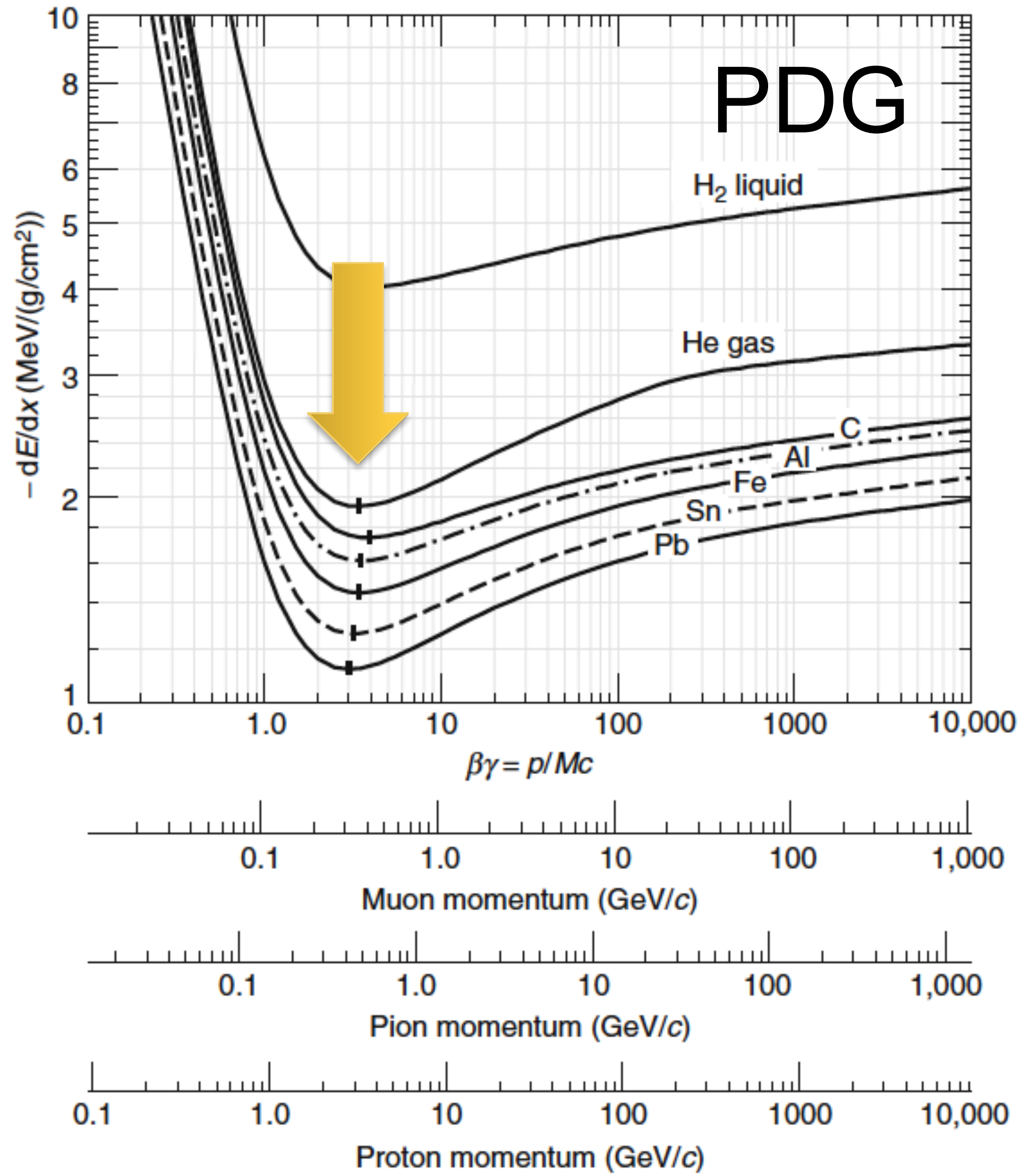

dE/dx Fluctuations

- The statistical nature of the ionizing process results in large fluctuations of energy loss (Δ

$$\Delta E = \sum_{n=1}^{N} \delta E_n$$

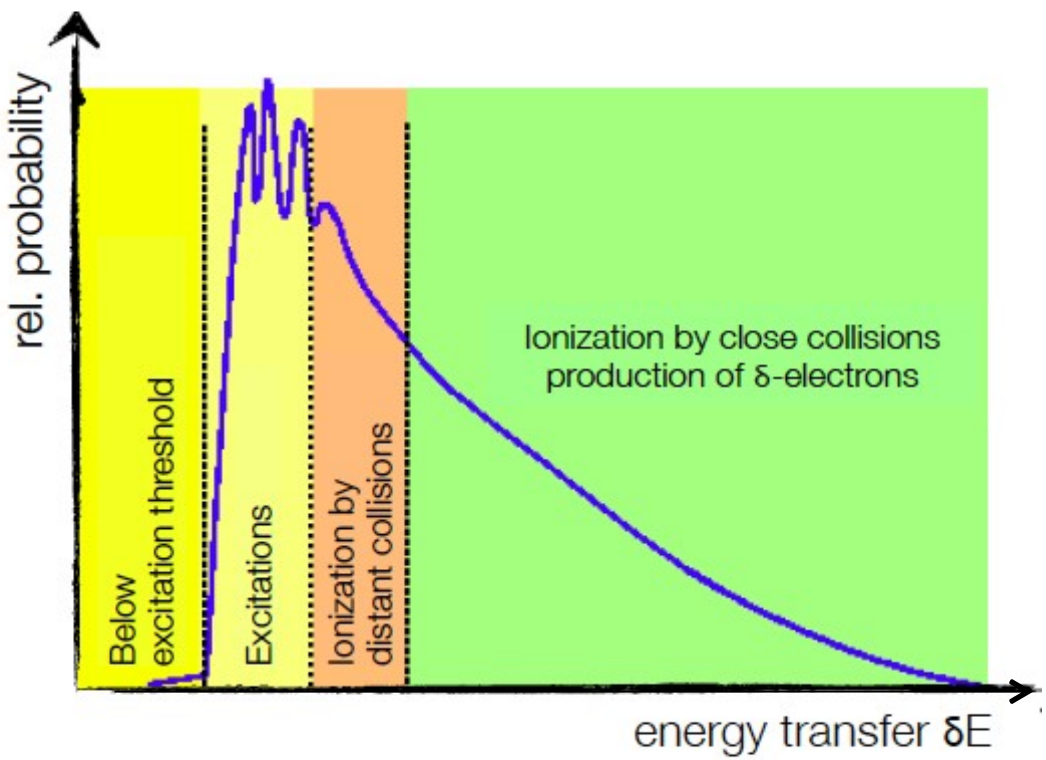

- Ionization loss is distributed statistically
- Small probability to have very high energy delta-rays (or knock-on electrons)

Landau tail

- Real detectors can not measure <dE/dx>
  - The energy ΔE deposited in a layer of finite thickness δx *is measured*.

- For thin layers of solids or low density materials:
  - Few collisions, some with high energy transfer.

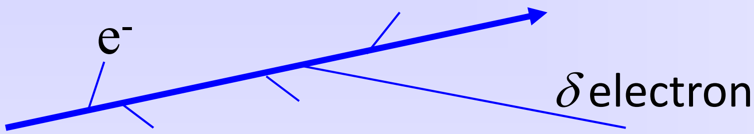

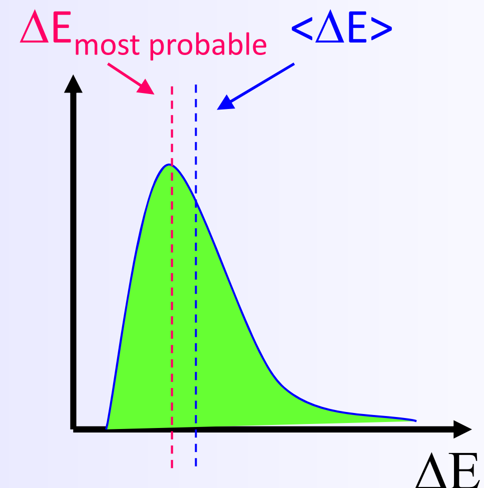

  - Energy loss distributions show large fluctuations towards high losses; Landau distribution with tails

Example: Si sensor: 300 μm thick. $\Delta E_{\text{most probable}} \sim 82$ keV $\quad \langle \Delta E \rangle \sim 115$ keV

- For thick layers and high density materials:
  - Many collisions
  - Central Limit Theorem ➔ Gaussian shaped distributions

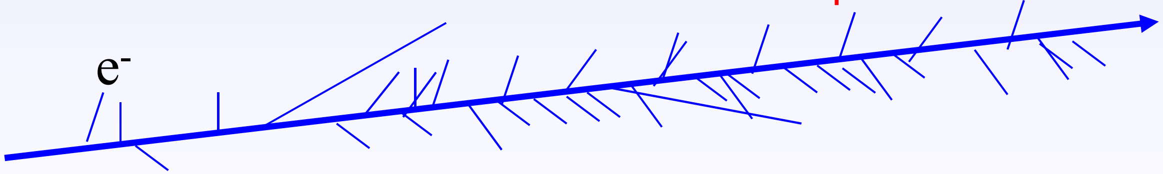

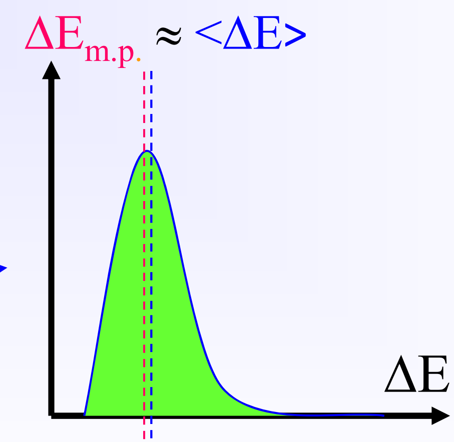

from Michael Moll lectures

Elastic scattering

- Most basic interaction of a charged particle in matter
  - elastic scattering with a nucleus
    = Rutherford (Coulomb) scattering
  - An incoming particle with charge z interacts elastically with a target of nuclear charge Z.

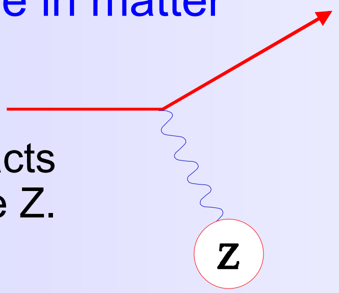

'The scattering of alpha and beta particles by matter and the structure of the atom', Philosophical Magazine, vol. 21 (1911), 669-688.

Ernest Rutherford
May 1911

Cross section for this e.m. process is given by the Rutherford formula:

$$\frac{d\sigma}{d\Omega} = 4zZr_e^2\left(\frac{m_e c}{\beta p}\right)^2 \frac{1}{\sin^4\theta/2}$$

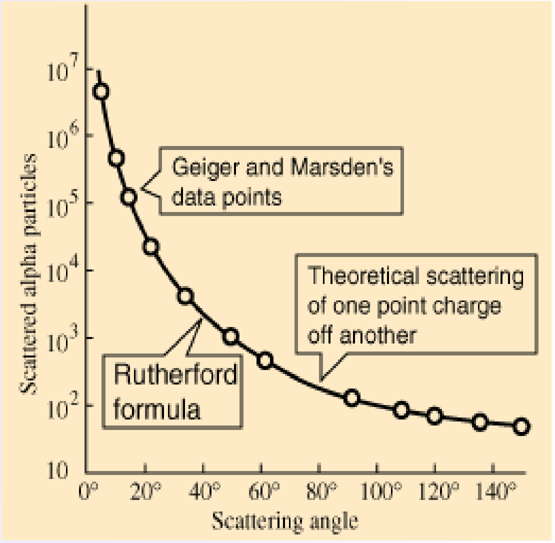

UK Science Museum

- Approximations
  - non-relativistic
  - no spins

- Scattering angle and energy transfer to nucleus usually small
  - No (significant) energy loss of the incoming particle
  - Just change of particle direction

from Michael Moll lectures

Multiple scattering

- In a sufficiently thick material layer a particle will undergo **multiple scattering**
  - **after passing material layer of thickness L particle leaves with some displacement r_{plane} and some deflection angle Θ_{plane}**

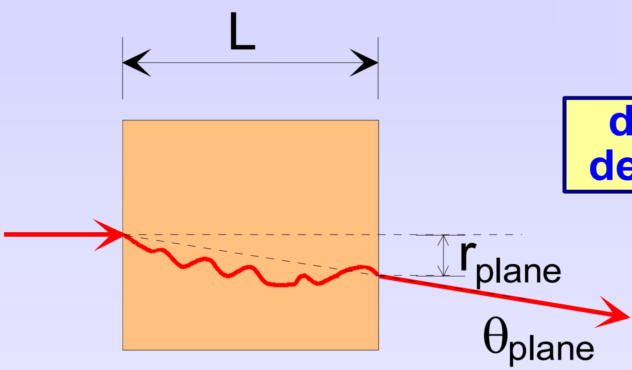

distribution of deflection angle

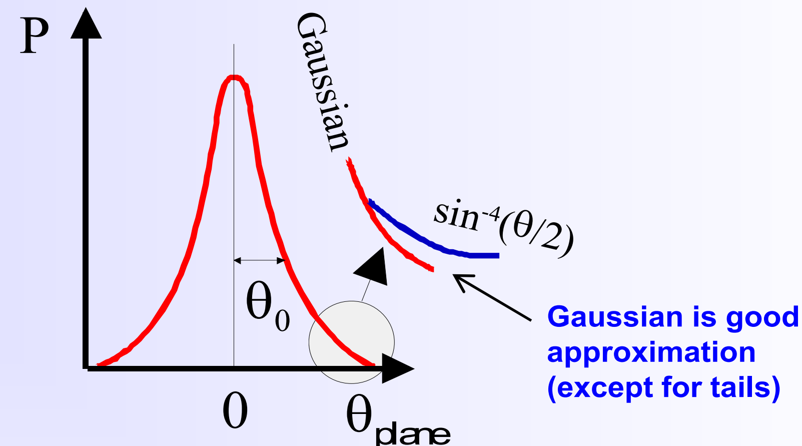

Θ_0 = width of distribution

$$\theta_0 \propto \frac{1}{p}\sqrt{\frac{L}{X_0}}$$

- Multiple scattering dominates the momentum measurement resolution for low momenta (see later)
  - X_0 = radiation length (see later)

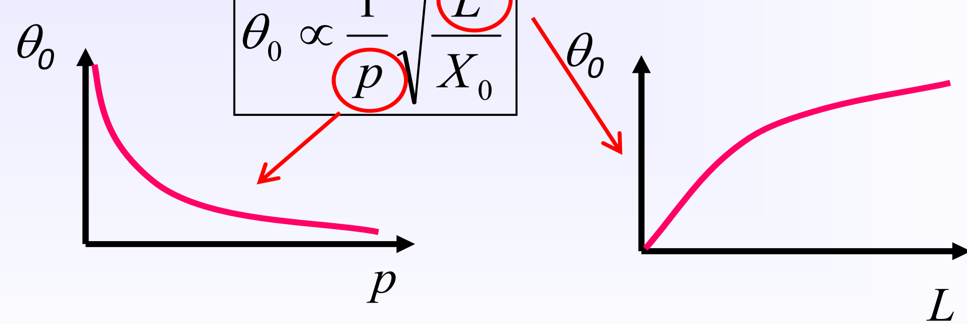

from Michael Moll lectures

Tracking and Vertex Detectors

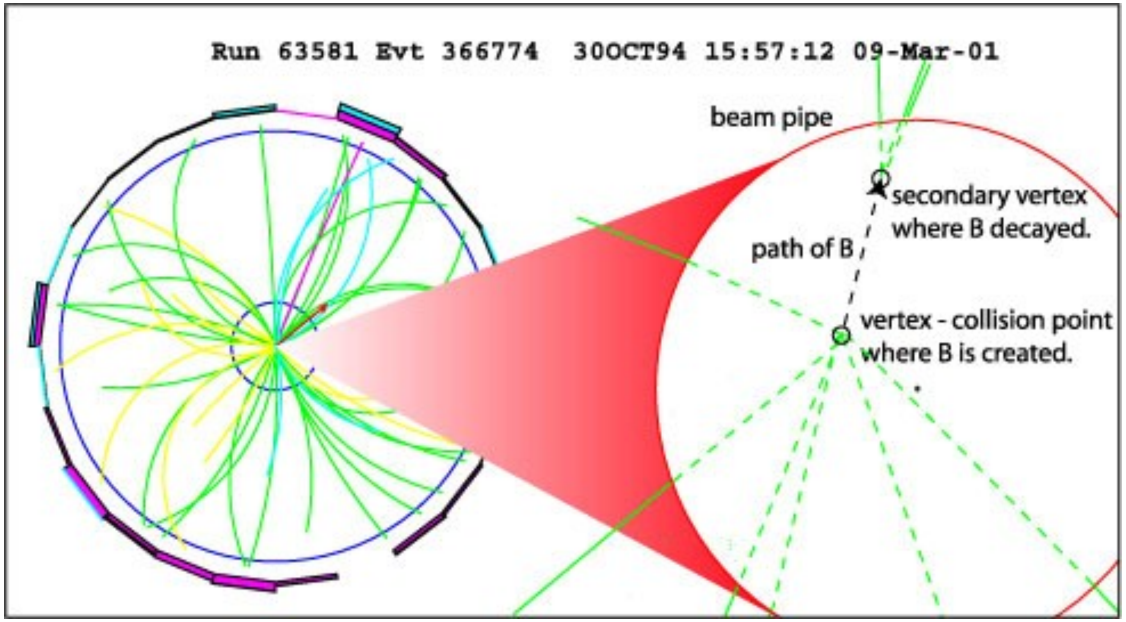

Tracking and Vertex Detectors

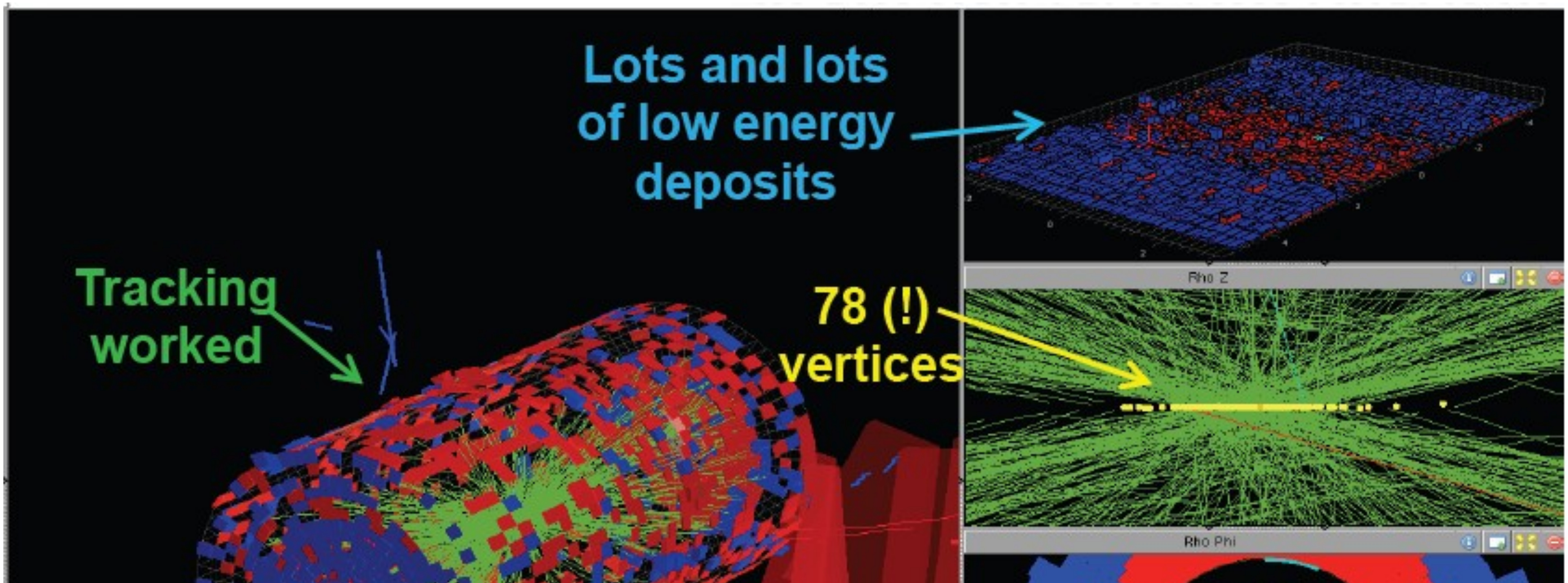

This would have not been possible without semiconductor (pixel and strip) trackers

Momentum measurement

- Moving charged particles are deflected by magnetic fields
  - In a homogeneous ***B*** field particle follows circle with radius ***r***

$$p_t[GeV/c] = 0.3 \cdot B[T] \cdot r[m]$$

  - $\boldsymbol{p_t}$ is the component of the momentum orthogonal to ***B*** field

p_t : transverse momentum

measurement of p_t via measuring the radius

Lorentz Force

$$\vec{F}_L = q \cdot \vec{v} \times \vec{B}$$

Centripetal Force

$$F_c = m \cdot v^2 / r$$

$$p = q \cdot B \cdot r$$

  - no particle deflection parallel to magnetic field
  - if particle has longitudinal momentum component, the particle will follow a helix

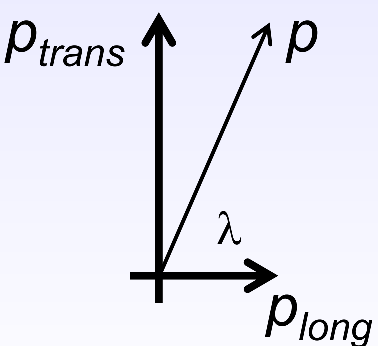

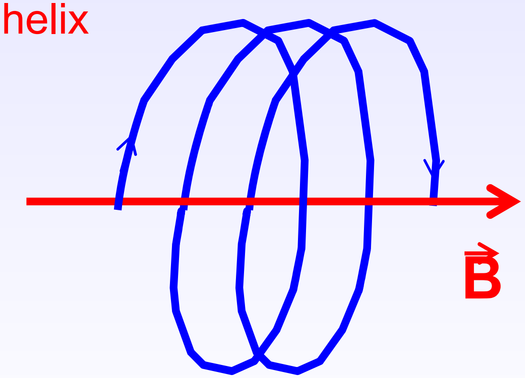

total momentum *p* to be measured via dip angle λ

$$p = \frac{p_t}{\sin \lambda}$$

from Michael Moll lectures

Momentum measurement error

- How to measure the radius r (curvature) ?
  - Tracking Detectors measure the positions of the track along various points along the track (circle)

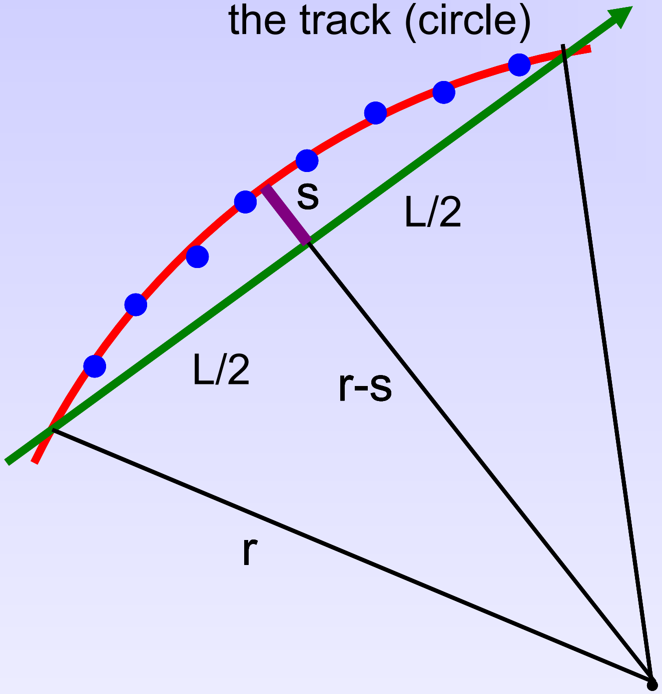

measure the sagitta s of the track

$$r = \frac{L^2}{8s} + \frac{s}{2} \quad \text{if } s \ll L \quad r \approx \frac{L^2}{8s}$$

sagitta s / radius r is obtained by a circle fit through measurement points along the track with point resolution $\sigma_{r\phi}$ for each point

sagitta error $$\sigma_S = \sqrt{\frac{A_N}{N+4}} \cdot \frac{\sigma_{r\phi}}{8}$$ with statistical factor $A_N = 720$

R.L. Gluckstern, NIM 24 (1963), 381

relative transverse momentum resolution σ_{pt}/p_t

- degrades linearly with momentum
- improves linearly with B field
- improves quadratically with radial extension of detector

$$\frac{\sigma_{p_T}}{p_T} = \frac{8 p_T}{0.3 B L^2} \cdot \sigma_S \quad \rightarrow \quad \frac{\sigma_{p_T}}{p_T} \propto p_T$$

from Michael Moll lectures

Momentum resolution

- The (transverse) momentum resolution is dominated by two contributions
  - **contribution from measurement error**

$$\frac{\sigma_{p_T}}{p_T} \propto p_T$$

  - **contribution form multiple scattering** (remember)

$$\theta_0 \propto \frac{1}{p_T}\sqrt{\frac{L}{X_0}} \qquad \sigma_{r\varphi}\Big|^{MS} \propto \theta_0 \qquad \frac{\sigma_{p_T}}{p_T} \propto p_T \cdot \sigma_{r\varphi}$$

$$\frac{\sigma_{p_T}}{p_T}\Bigg|^{MS} = \text{constant}$$

multiple scattering contribution to the transverse momentum error is constant (i.e. independent of the momentum)

More precise:

$$\frac{\sigma(p_T)}{p_T}\Bigg|^{MS} = 0.045\frac{1}{B\sqrt{LX_0}}$$

Example: Detector (L=1m) filled with 1atm Argon gas (X_0=110m); B=1T

$$\frac{\sigma(p_T)}{p_T}\Bigg|^{MS} = 0.5\%$$

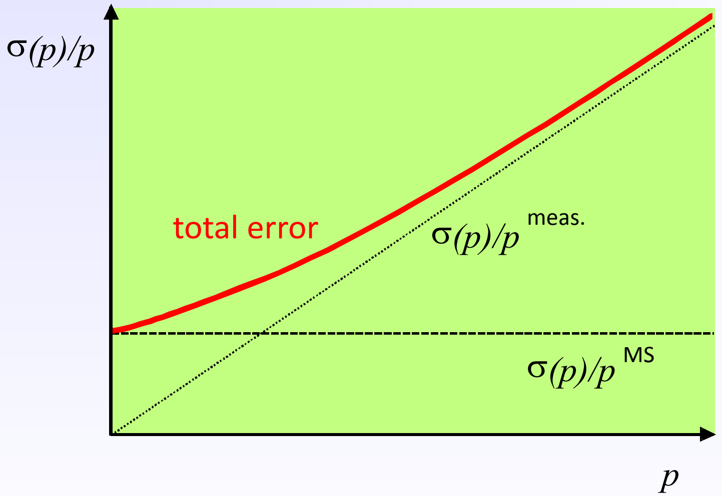

from Michael Moll lectures

Impact parameter resolution

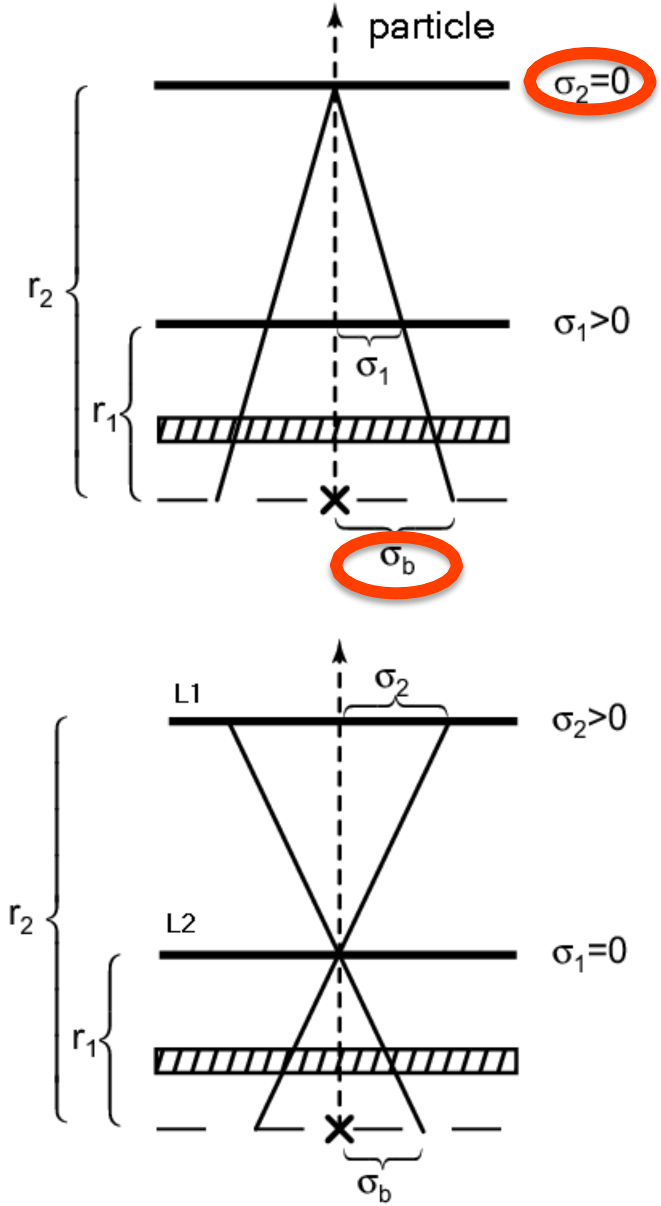

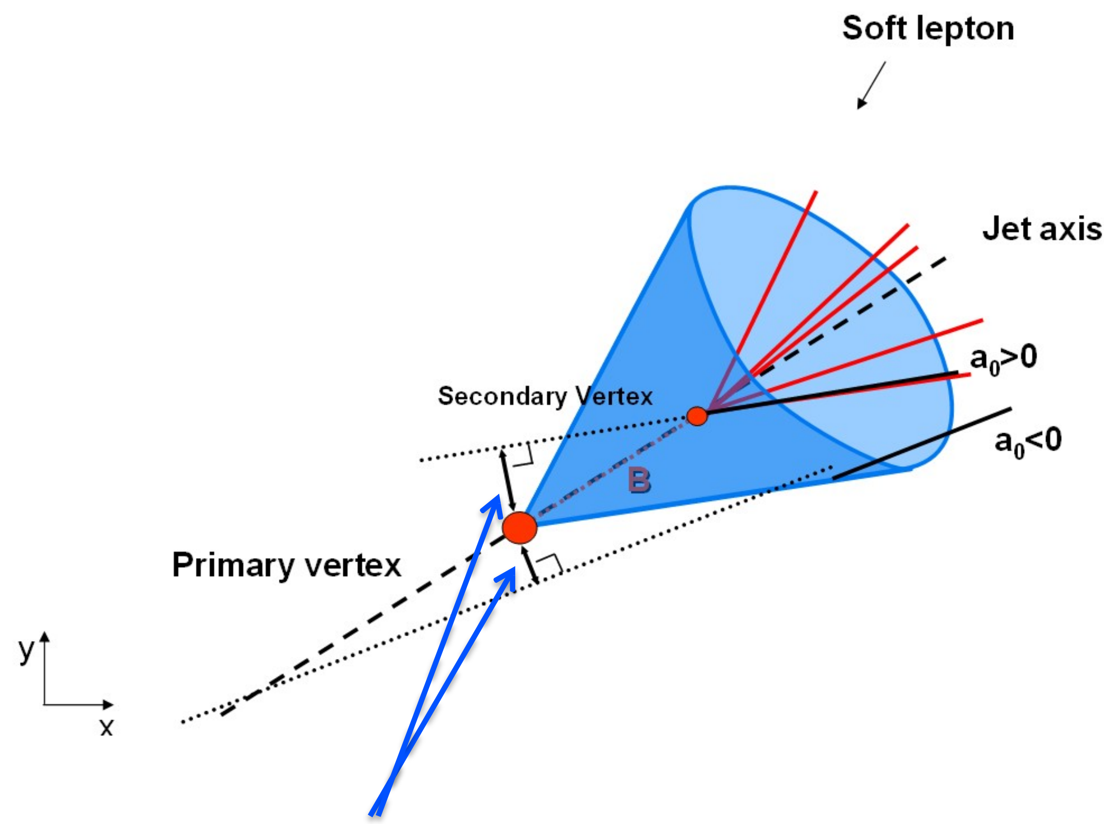

Impact parameter resolution

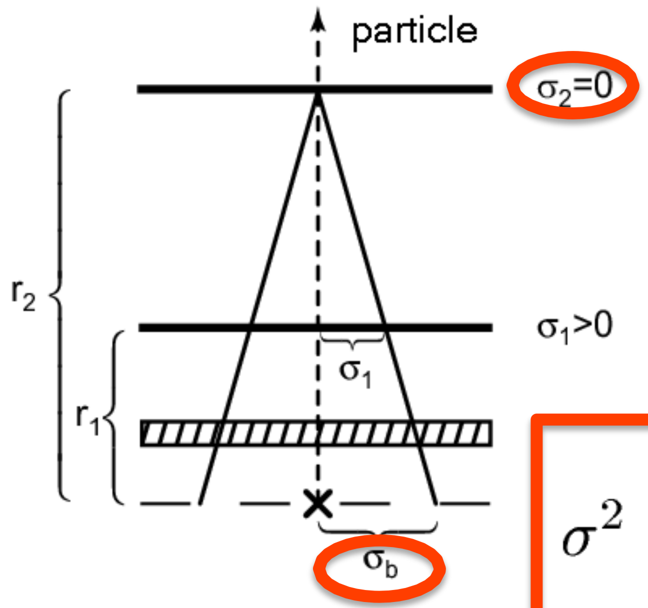

$$\frac{\sigma_b}{\sigma_1} = \frac{r_2}{r_2 - r_1}$$

$$\sigma^2 = \left(\frac{r_1}{r_2 - r_1}\sigma_2\right)^2 + \left(\frac{r_2}{r_2 - r_1}\sigma_1\right)^2 + \sigma_{MS}^2$$

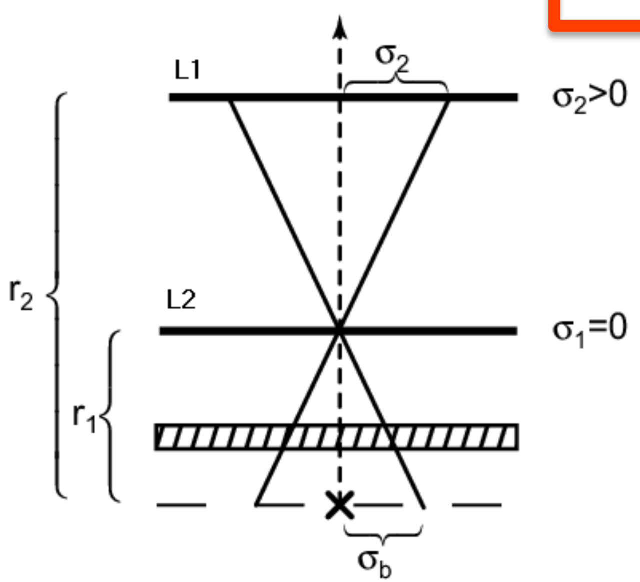

$$\frac{\sigma_b}{\sigma_2} = \frac{r_1}{r_2 - r_1}$$

$$\sigma_{MS} \sim \frac{1}{p}\sqrt{\frac{x}{X_0}}$$

Precision measurements at small radii

- A solid state detector is an ionization chamber
  - Ionizing radiation creates electron/hole pairs
  - Charge carriers move in applied E field
  - Motion induces a current in an external circuit, which can be amplified and sensed.

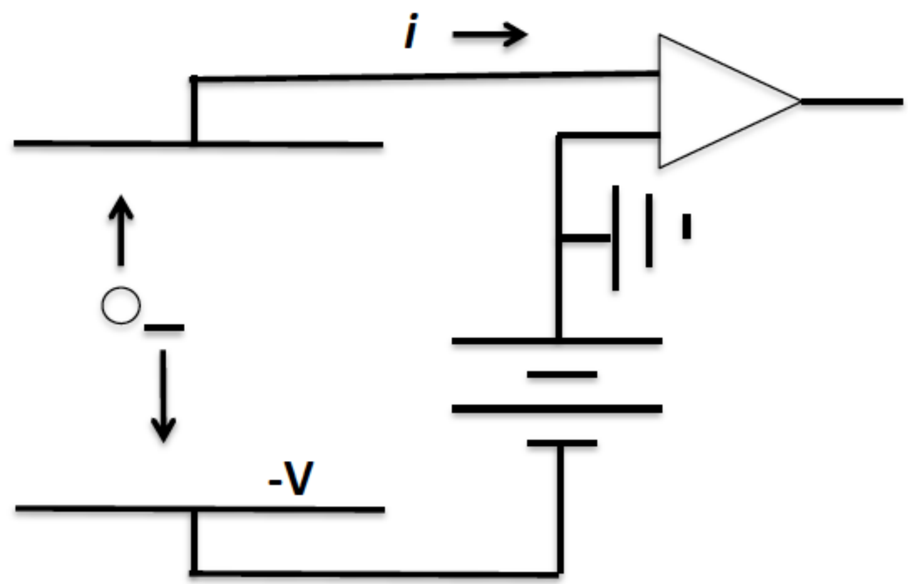

	Gas	Solid
Density	**Low**	High
Atomic number (Z)	Low	Moderate
Ionization Energy (ε_I)	Moderate (≈ 30 eV)	Low (≈3.6 eV)
Signal Speed	Moderate (10ns-10μs)	Fast (<20 ns)

Double Sided Silicon Detectors

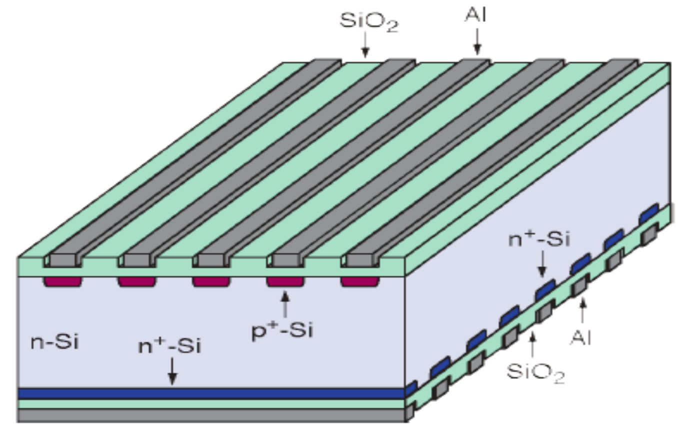

Scheme of a double sided strip detector
(biasing structures not shown)

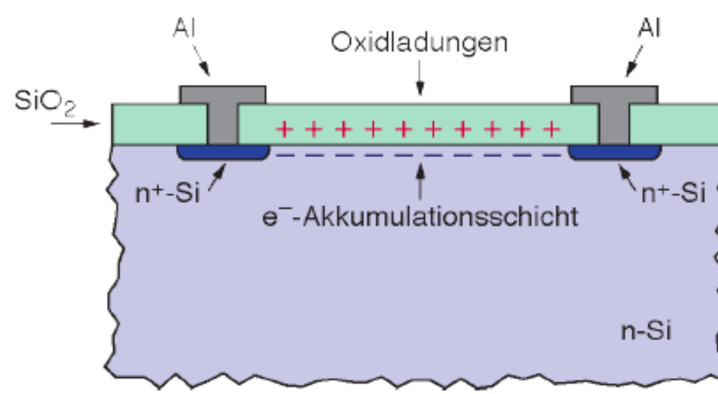

Positive oxide charges cause electron accumulation layer.

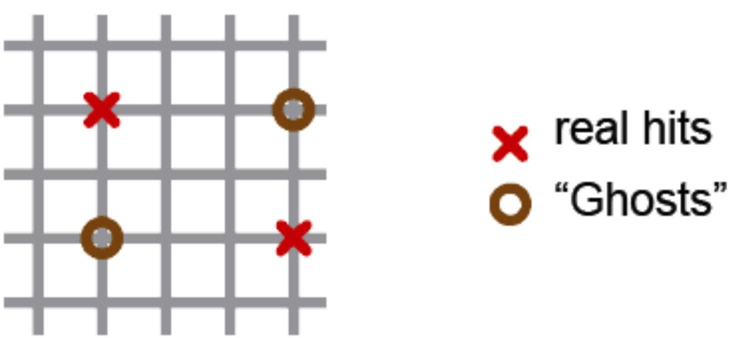

Pixel detector

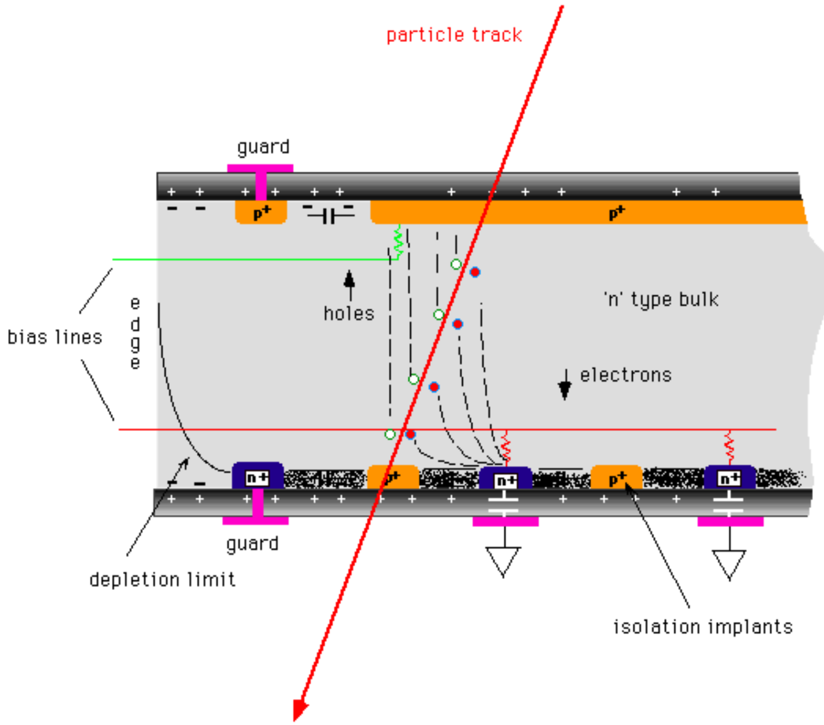

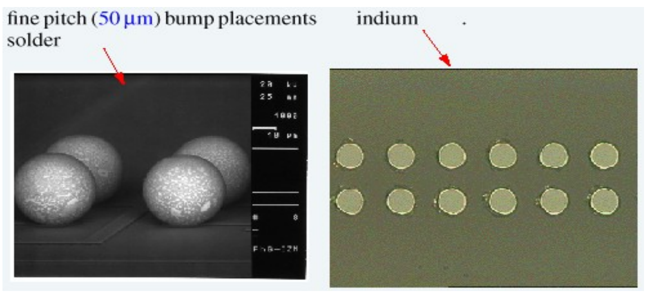

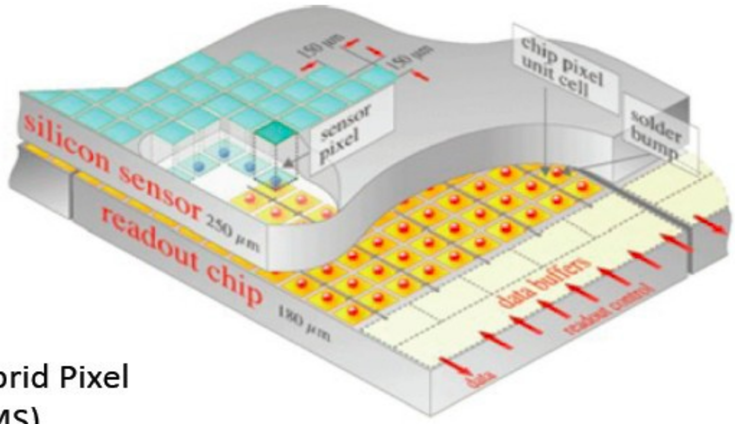

Hybrid Pixel
(CMS)

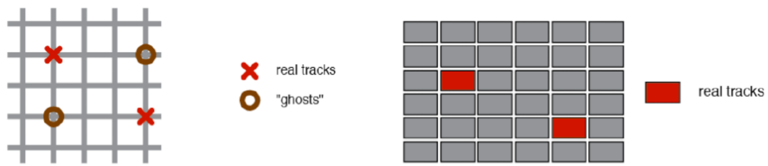

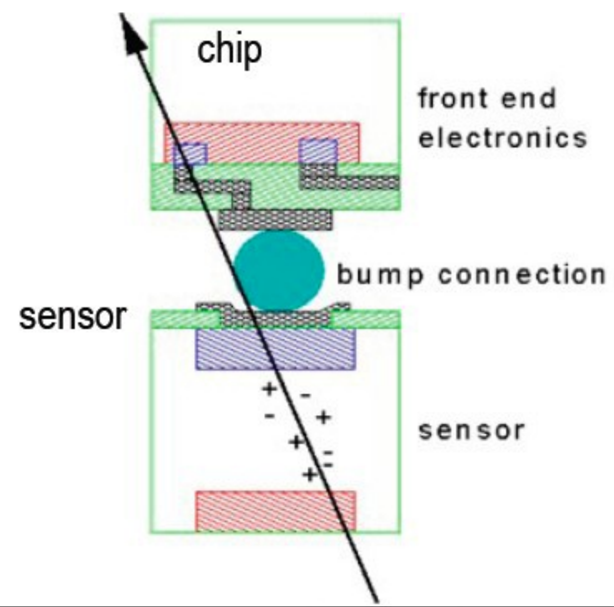

https://www.youtube.com/watch?v=ojeVwQxOrGo&feature=youtu.be

Most probable charge ≈ 0.7×mean

Mean charge

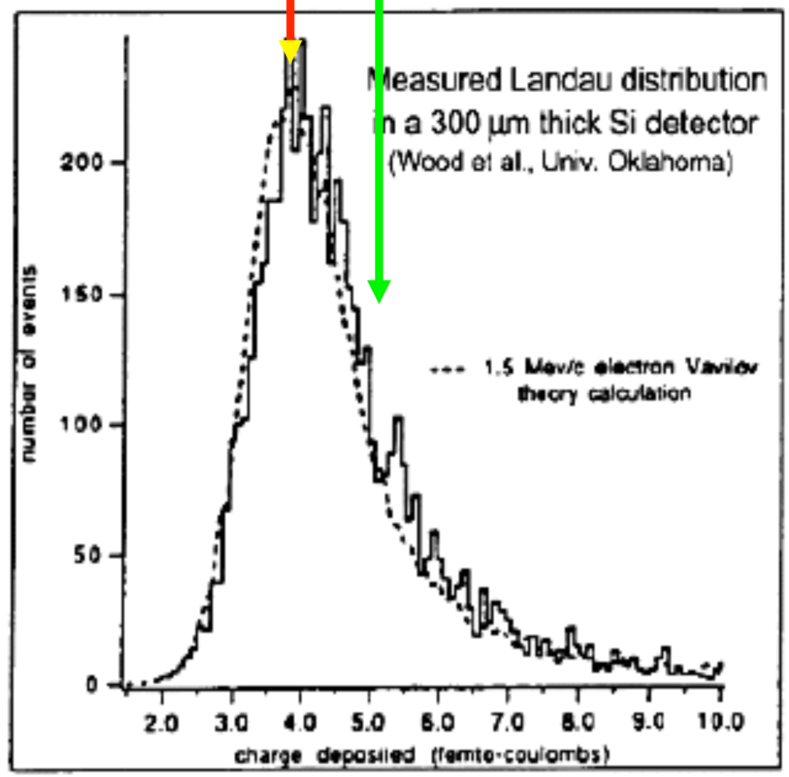

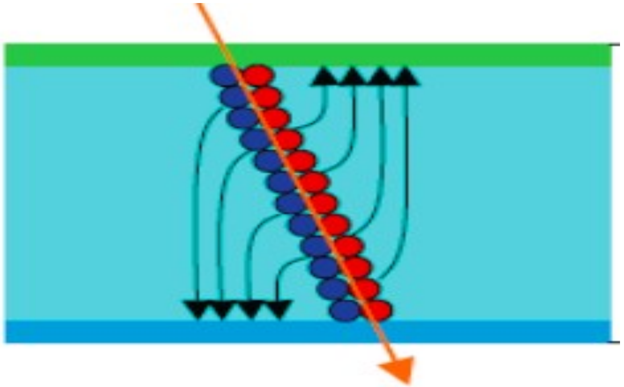

$$\mathrm{ENC} = \frac{\text{noise output voltage (rms)}}{\text{signal output voltage for the input charge of } 1\mathrm{e}^-}$$

$$ENC_{tot}^2 = ENC_{shot}^2 + ENC_{therm}^2 + ENC_{1/f}^2$$

Reference
Rossi, Fischer, Rohe, Wermes
Pixel Detectors

$$ENC_{\text{shot}} = \sqrt{\frac{I_{leak}}{2q}\tau_f} = 56e^- \times \sqrt{\frac{I_{\text{leak}}}{\text{n}A}\frac{\tau_f}{\mu s}}$$

$$ENC_{\text{therm}} = \frac{C_f}{q}\sqrt{\langle v_{\text{therm}}^2\rangle} = \sqrt{\frac{kT}{q}\frac{2C_D}{3q}\frac{C_f}{C_{load}}} = 104e^- \times \sqrt{\frac{C_D}{100\,\text{fF}}\frac{C_f}{C_{load}}}$$

$$ENC_{1/\text{f}} \approx \frac{C_D}{q}\sqrt{\frac{K_f}{C_{ox}WL}}\sqrt{\ln\left(\tau_f \frac{g_m}{C_{load}}\frac{C_f}{C_D}\right)} = 9e^- \times \frac{C_D}{100\,\text{fF}} (\text{for NMOS trans.})$$

W, L = width and length of trans. gate
K_f = 1/f noise coefficient
C_{ox} = gate oxide capacitance

C_f = feedback capacitance
C_{load} = load capacitance
C_D = detector capacitance
τ_f = feedback time constant

Diffusion

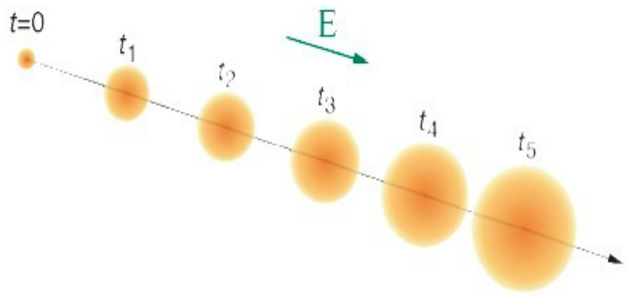

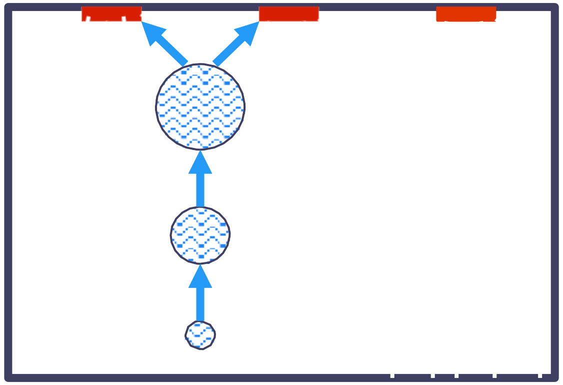

Charge density distribution for 5 equidistant time intervalls:

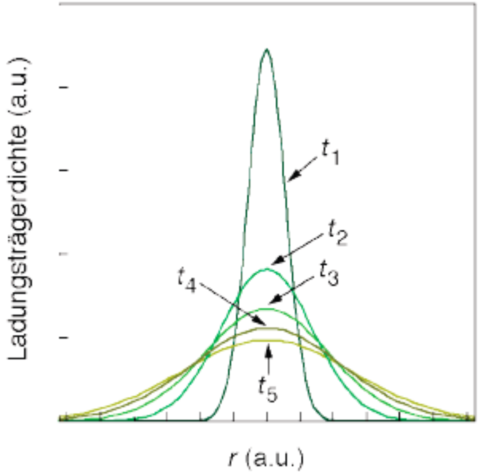

Position resolution

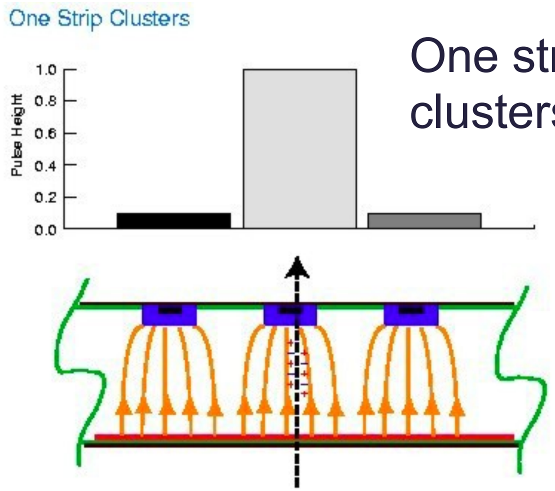

One strip clusters

$$\sigma = \frac{pitch}{\sqrt{12}}$$

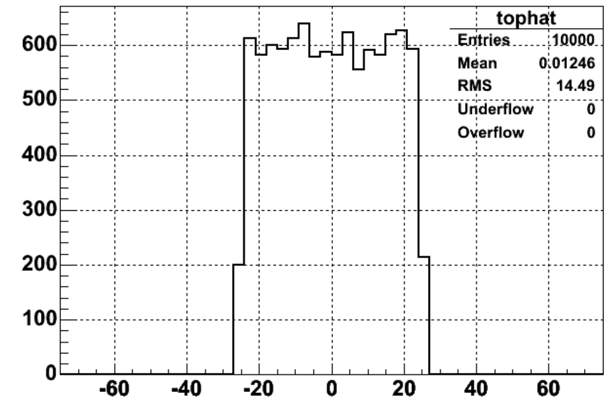

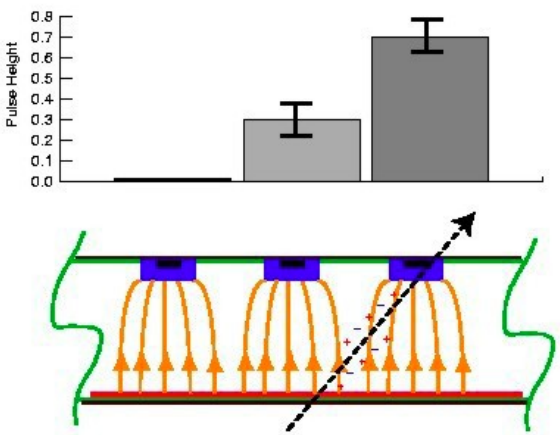

$$\sigma \approx \frac{pitch}{1.5 \cdot \sqrt{12}}$$

$$\eta = \frac{PH_R}{PH_L + PH_R}$$

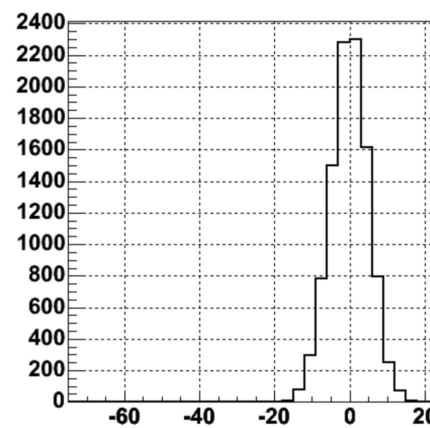

Charge sharing

Momentum measurement

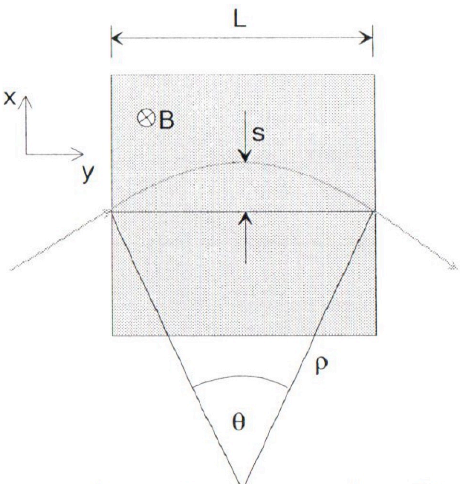

$$\frac{mv^2}{\rho} = q(v \times B) \quad \rightarrow \quad p_T = qB\rho$$

$$p_T \text{ (GeV/c)} = 0.3B\rho \quad (\text{T} \cdot \text{m})$$

$$\frac{L}{2\rho} = \sin\theta/2 \approx \theta/2 \quad \rightarrow \quad \theta \approx \frac{0.3L \cdot B}{p_T}$$

sagitta $$s = \rho(1 - \cos\theta/2) \approx \rho\frac{\theta^2}{8} \approx \frac{0.3}{8}\frac{L^2 B}{p_T}$$

The sagitta s is determined by 3 measurements with error *s(x):*

Error on the sagitta $$s = x_2 - \tfrac{1}{2}(x_1 + x_3)$$

$$\left.\frac{\sigma(p_T)}{p_T}\right|^{meas.} = \frac{\sigma(s)}{s} = \frac{\sqrt{\frac{3}{2}}\sigma(x)}{s} = \frac{\sqrt{\frac{3}{2}}\sigma(x) \cdot 8p_T}{0.3 \cdot BL^2}$$

Can we distinguish curved track from the straight line ?

$s = r - \sqrt{(r^2 - L^2/4)}$

CLEO (electron-positron collider):

Maximum momentum p = 5 GeV/c, B field = 1.5 T

→ r = p/(0.3 B) = 11.11 m

Track radius = 1.0 m

→s = 0.011 m (1.1 mm) **EASY !!!**

ATLAS

Tracking length L = 1.15 m

B field = 2 T

p = 50 GeV/c r = 144.9 m s = 1.1 mm

p = 1000 GeV/c r= 1666.7 m s = 100 m !!!!

⇨ **must consider measurement errors**